

AD-A158 979

NAVAL POSTGRADUATE SCHOOL

Monterey, California



THESIS

DETECTION OF PERIODIC SIGNAL OF ARBITRARY
SHAPE WITH RANDOM TIME DELAY

by

Khalil Ahmed Ansari

June 1985

Thesis Advisor:

Daniel Bukofzer

DTIC FILE COPY

DTIC
ELECTE
SEP 13 1985

A

Approved for public release; distribution is unlimited

85 9 10 09 1

UNCLASSIFIED

SECURITY CLASSIFICATION OF THIS PAGE (When Data Entered)

REPORT DOCUMENTATION PAGE		READ INSTRUCTIONS BEFORE COMPLETING FORM
1. REPORT NUMBER	2. GOVT ACCESSION NO. AD-A158979	3. RECIPIENT'S CATALOG NUMBER
4. TITLE (and Subtitle) Detection of Periodic Signal of Arbitrary Shape with Random Time Delay		5. TYPE OF REPORT & PERIOD COVERED Master's Thesis June 1985
7. AUTHOR(s) Khalil Ahmed Ansari		6. PERFORMING ORG. REPORT NUMBER
9. PERFORMING ORGANIZATION NAME AND ADDRESS Naval Postgraduate School Monterey, California 93943-5100		8. CONTRACT OR GRANT NUMBER(s)
11. CONTROLLING OFFICE NAME AND ADDRESS Naval Postgraduate School Monterey, California 93943-5100		10. PROGRAM ELEMENT, PROJECT, TASK AREA & WORK UNIT NUMBERS
14. MONITORING AGENCY NAME & ADDRESS (if different from Controlling Office)		12. REPORT DATE June 1985
		13. NUMBER OF PAGES 112
		15. SECURITY CLASS. (of this report) Unclassified
		15a. DECLASSIFICATION/DOWNGRADING SCHEDULE
16. DISTRIBUTION STATEMENT (of this Report) Approved for public release; distribution is unlimited		
17. DISTRIBUTION STATEMENT (of the abstract entered in Block 20, if different from Report)		
18. SUPPLEMENTARY NOTES		
19. KEY WORDS (Continue on reverse side if necessary and identify by block number) Noncoherent Receiver Design; Random Time Delay; Periodic Signal		
20. ABSTRACT (Continue on reverse side if necessary and identify by block number) The detection of periodic signals of arbitrary wave shape with random time delay in additive white Gaussian noise, is a problem of practical significance in radar and communication applications. In this thesis, the analysis and design of optimum and suboptimum receivers for detecting signals as described above has been carried out. The design of optimum (in minimum		

DD FORM 1473
1 JAN 73EDITION OF 1 NOV 65 IS OBSOLETE
S N 0102-LF-014-6601

1

UNCLASSIFIED

SECURITY CLASSIFICATION OF THIS PAGE (When Data Entered)

UNCLASSIFIED

SECURITY CLASSIFICATION OF THIS PAGE (When Data Entered)

#20 - ABSTRACT - (CONTINUED)

probability of error, P_e sense) receivers is based on the likelihood ratio test under the assumption of low SNR conditions. The design of suboptimum receivers is based on the heuristic approaches that intuitively yield reasonably good performance. Examples have been analyzed in order to present numerical results in graphical form on the performance of the receivers under different assumptions of wave shapes and p.d.f. on the random time delay associated with the signal.

UNCLASSIFIED

SECURITY CLASSIFICATION OF THIS PAGE(When Data Entered)

Approved for public release; distribution unlimited.

Detection of Periodic Signal of Arbitrary
Shape with Random Time Delay

by

Khalil Ahmed Ansari
Lieutenant, Pakistan Navy
B.Engg., NED University of Engineering and Technology, 1979

Submitted in partial fulfillment of the
requirements for the degree of

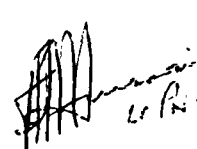
MASTER OF SCIENCE IN ELECTRICAL ENGINEERING

from the

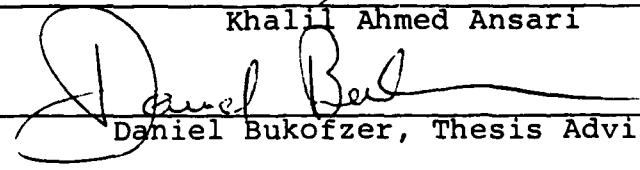
NAVAL POSTGRADUATE SCHOOL

June 1985

Author:



Khalil Ahmed Ansari

Approved by:


Daniel Bukofzer, Thesis Advisor

Jin F. Chang, Second Reader

Harriett B. Rigas, Chairman,
Department of Electrical and Computer Engineering


J.N. Dyer, Dean of Science and Engineering



A1

ABSTRACT

The detection of periodic signals of arbitrary wave shape with random time delay in additive white Gaussian noise, is a problem of practical significance in radar and communication applications.

In this thesis, the analysis and design of optimum and suboptimum receivers for detecting signals as described above has been carried out. The design of optimum (in minimum probability of error, P_e sense) receivers is based on the likelihood ratio test under the assumption of low SNR conditions. The design of suboptimum receivers is based on heuristic approaches that intuitively yield reasonably good performance. Examples have been analyzed in order to present numerical results in graphical form on the performance of the receivers under different assumptions of wave shapes and p.d.f. on the random time delay associated with the signal.

TABLE OF CONTENTS

I.	INTRODUCTION -----	11
II.	NONCOHERENT RECEIVER ANALYSIS -----	14
	A. BASIC CONCEPT -----	14
	B. PROBABILITY DENSITY FUNCTION OF λ -----	15
	C. COMPUTATION OF LIKELIHOOD RATIO -----	17
	D. TWO TERM APPROXIMATION -----	22
	1. Uniform p.d.f. -----	23
	2. Nonuniform p.d.f. -----	29
	E. THREE TERM APPROXIMATION -----	36
	1. Uniform p.d.f. -----	37
	2. Nonuniform p.d.f. -----	38
	F. ANALYSIS OF TWO SPECIFIC SIGNAL WAVE SHAPES -	43
	1. Sine Wave -----	44
	2. Square Wave -----	45
	G. DISCUSSION -----	49
III.	ALTERNATIVE SUBOPTIMUM RECEIVERS -----	50
	A. N-CORRELATOR RECEIVER -----	50
	1. Special Case of Triangular Wave -----	57
	B. ESTIMATOR-CORRELATOR RECEIVER -----	69
	1. Special Case of Sine Wave -----	75
	2. Special Case of Square Wave -----	76
IV.	DISCUSSION OF GRAPHICAL RESULTS -----	79
	A. GRAPHICAL RESULTS FOR OPTIMUM RECEIVERS -----	79

1. Receiver Operating on Signals with Nonzero DC Component (Uniform p.d.f. on λ) -----	79
2. Receiver Operating on Arbitrary Signals (Nonuniform p.d.f. on λ) -----	81
B. GRAPHICAL RESULTS FOR SUBOPTIMUM RECEIVERS --	85
1. N-Correlator Receiver -----	86
2. Estimator-Correlator Receiver -----	87
V. CONCLUSIONS -----	103
APPENDIX A: DERIVATION OF MEAN AND VARIANCE OF R.V. λ -----	106
APPENDIX B: INTERPRETATION OF A SMALL EXPONENTIAL IN EQUATION (2.22) AND EQUATION (2.60) ---	108
LIST OF REFERENCES -----	111
INITIAL DISTRIBUTION LIST -----	112

LIST OF TABLES

I. Probability of Error versus # of Coefficients	
Summed -----	85

LIST OF FIGURES

2.1	PDF of Time Delay -----	16
2.2	Noncoherent Receiver (Uniform p.d.f., 2 Term Approximation) -----	24
2.3	Probability Density Function of λ -----	27
2.4	Noncoherent Receiver (Nonuniform p.d.f., 2 Term Approximation) -----	32
2.5	Noncoherent Receiver (Uniform p.d.f., 3 Term Approximation) -----	39
2.6	Noncoherent Receiver (Nonuniform p.d.f., 3 Term Approximation) -----	42
2.7	Periodic Square Wave -----	46
3.1	N-Correlator Receiver -----	51
3.2	Periodic Triangular Wave and Two of Its Delayed Versions -----	58
3.3	One Period Restricted Triangular Wave and Two of Its Delayed Versions -----	59
3.4	Estimator-Correlator Receiver -----	70
4.1	Performance (Uniform p.d.f.) -----	80
4.2	Performance (Sine Wave) -----	83
4.3	Performance (Square Wave) -----	84
4.4	P_e vs Thld ($m = 0, N = 16$), (SNR = -10, -5, 0, 5 dB) -----	88
4.5	P_e vs Thld ($m = 0, N = 16$), (SNR = 10, 15, 16.5 dB) -----	89
4.6	P_e vs Thld ($m = 30, N = 16$), (SNR = -10, -5, 0, 5 dB) -----	90
4.7	P_e vs Thld ($m = 30, N = 16$), (SNR = 10, 15, 16.5 dB) -----	91

4.8	P_e vs Thld ($m = 0, N = 2$), (SNR = -10, -5, 0, 5 dB) -----	92
4.9	P_e vs Thld ($m = 0, N = 2$), (SNR = 10, 15, 16.5, 17 dB) -----	93
4.10	P_e vs Thld ($m = 30, N = 2$), (SNR = -10, -5, 0, 5 dB) -----	94
4.11	P_e vs Thld ($m = 30, N = 2$), (SNR = 10, 15, 16.5, 17 dB) -----	95
4.12	Performance (Triangular Pulse) -----	96
4.13	Performance (Sine Wave), ($\alpha = 0$) -----	99
4.14	Performance (Sine Wave), ($\alpha = T/2$) -----	100
4.15	Performance (Square Wave), ($\alpha = 0$) -----	101
4.16	Performance (Square Wave), ($\alpha = T/2$) -----	102

ACKNOWLEDGEMENT

I wish to gratefully express my appreciation to my thesis advisor, Prof. Daniel Bukofzer, for his invaluable efforts and patience in assisting me throughout my research.

I. INTRODUCTION

Classical noncoherent signal detection is generally understood to mean the detection of a sine wave with random phase or time delay in additive white Gaussian noise (WGN). However, the extension of this problem to a general noncoherent problem involving the detection of an arbitrary periodic signal with random time delay in additive WGN, has received little attention. A case of particular practical interest involves the detection of a baseband square wave with random time delay in additive WGN.

In digital communication systems, the message to be transmitted is encoded into a sequence of binary digits. Typically, these digits represented by the logical states '1' and '0' are transmitted by sending a suitably chosen set of pulses which are distorted during both transmission and reception. The effect of this distortion is that at the receiver, it is no longer possible to determine exactly which waveform was actually transmitted. We can model the transmission as well as the distortion introduced in the receiver itself, as random noise. In all the analysis carried out, it will be assumed that the random noise can be modeled as additive, white Gaussian. The problem then is one of deciding, on the basis of noisy observations, whether the transmitted waveform corresponds to a logical '1' or a logical '0'.

In this thesis, the analysis and design of noncoherent receivers that optimally (and in some cases suboptimally)

It is clear from Equation (2.30) that this simple receiver can only operate provided $V_0 \neq 0$. If V_0 is indeed zero, some other approach must be used for the purpose of deciding on which hypothesis is true upon reception of $r(t)$. In the sequel we discuss other detection approaches which will work even if $V_0 = 0$.

The performance of this receiver is evaluated as follows.

Let

$$\ell = V_0 \int_0^{T_0} r(t) dt \quad (2.31)$$

Conditioning on λ , we see that ℓ is a conditional Gaussian random variable, where

$$E\{\ell | H_0\} = 0 \triangleq m_0 \quad (2.32)$$

$$\begin{aligned} E\{\ell | H_1, \lambda\} &= V_0 \int_0^{T_0} v(t-\lambda) dt \\ &= V_0 \sum_{k=-\infty}^{\infty} V_k e^{-j\frac{2\pi k}{T}\lambda} \int_0^{T_0} e^{j\frac{2\pi k}{T}t} dt \\ &= V_0^2 T_0 \triangleq m_1 \end{aligned} \quad (2.33)$$

Furthermore

However, since

$$\int_{-T/2}^{T/2} e^{-j\frac{2\pi k}{T}\lambda} d\lambda = \begin{cases} T & \text{if } k = 0 \\ 0 & \text{otherwise} \end{cases} \quad (2.27)$$

the test of Equation (2.26) reduces to

$$V_0 R_0 \begin{matrix} H_1 \\ > \\ < \\ H_0 \end{matrix} \eta_* \quad (2.28)$$

where V_0 is just the d.c. component of $v(t)$. Note that for $k = 0$, Equation (2.18) becomes

$$R_0 = \int_0^{T_0} r(t) dt \quad (2.29)$$

so that the test can be expressed as

$$\int_0^{T_0} r(t) dt \begin{matrix} H_1 \\ > \\ < \\ H_0 \end{matrix} \eta_*/V_0 \quad (2.30)$$

and the receiver structure takes on the simple form shown in Fig. 2.2.

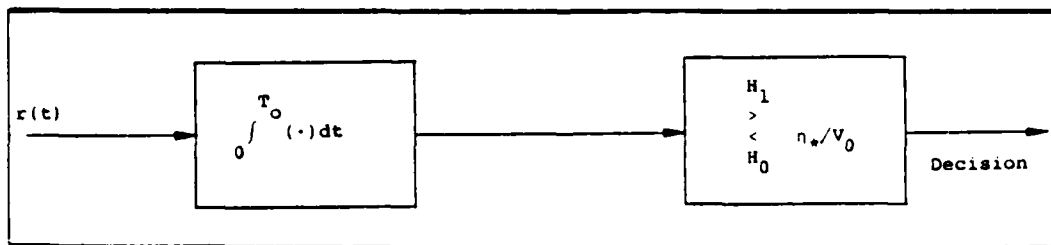


Figure 2.2 Noncoherent Receiver (Uniform p.d.f., 2 Term Approximation)

The test of Equation (2.23) is valid provided Equation (2.20) holds.

Observe that in order to limit the approximation error to 10% in Equation (2.21), $|x| \leq 0.39$.

In the remaining analysis we assume equal prior probabilities, namely $P\{H_0\} = \frac{1}{2} = P\{H_1\}$ and cost assignment $C_{ij} = 1 - \delta_{ij}$, so the threshold of Equation (2.23) becomes

$$\eta_* = \frac{N_0}{2} [e^{E/N_0} - 1] \quad (2.24)$$

In order to further analyze the test of Equation (2.23), we consider the following two cases:

1. Uniform p.d.f. on λ
2. Nonuniform p.d.f. on λ

1. Uniform p.d.f.

For this case, the p.d.f. of λ is

$$f_{\Lambda}(\lambda) = \frac{1}{T} \quad \lambda \leq |T/2| \quad (2.25)$$

and the test becomes

$$\frac{1}{T} \sum_{k=-\infty}^{\infty} V_k R_k \int_{-T/2}^{T/2} e^{-j \frac{2\pi k}{T} \lambda} d\lambda \begin{matrix} H_1 \\ > \\ < \\ H_0 \end{matrix} \eta_* \quad (2.26)$$

D. TWO TERM APPROXIMATION

In order to proceed with the analysis so as to derive a signal processing algorithm from Equation (2.19), we will assume that

$$\frac{2}{N_0} \sum_{k=-\infty}^{\infty} V_k R_k e^{-j \frac{2\pi k}{T} \lambda} \ll 1 \quad (2.20)$$

In Appendix B, we will show under what conditions this assumption is valid. It turns out that the assumption of Equation (2.20) is essentially equivalent to an assumption of low SNR, i.e., $E/N_0 \ll 1$.

Since

$$e^x \approx 1 + x \quad \text{if} \quad x \ll 1 \quad (2.21)$$

provided Equation (2.20) is valid, it is possible to approximate the exponential term of Equation (2.19) by two terms only so that the test can be written as

$$\int_{-\infty}^{\infty} \left(1 + \frac{2}{N_0} \sum_{k=-\infty}^{\infty} V_k R_k e^{-j \frac{2\pi k}{T} \lambda} \right) f_{\Lambda}(\lambda) d\lambda \underset{H_0}{\overset{H_1}{>}} n \exp\{E/N_0\} \quad (2.22)$$

or equivalently

$$\sum_{k=-\infty}^{\infty} V_k R_k \int_{-\infty}^{\infty} e^{-j \frac{2\pi k}{T} \lambda} f_{\Lambda}(\lambda) d\lambda \underset{H_0}{\overset{H_1}{>}} \frac{N_0}{2} [n \exp\{E/N_0\} - 1] \triangleq n_{*} \quad (2.23)$$

provided that $T_0 = nT$, where n is an integer. This result is also valid even if n is not an integer, provided that $n \gg 1$. Thus applying this result to Eq. (2.14) results in

$$\int_0^{T_0} v^2(t-\lambda) dt = T_0 \sum_{k=-\infty}^{\infty} v_k v_k^* = T_0 \sum_{k=-\infty}^{\infty} |v_k|^2 \triangleq E \quad (2.16)$$

Observe that E is the energy of the signal $v(t)$ for $0 \leq t \leq T_0$. Furthermore,

$$\begin{aligned} \int_0^{T_0} r(t) v(t-\lambda) dt &= \sum_{k=-\infty}^{\infty} v_k e^{-j\frac{2\pi}{T}k\lambda} \int_0^{T_0} r(t) e^{j\frac{2\pi}{T}kt} dt \\ &= \sum_{k=-\infty}^{\infty} v_k R_k e^{-j\frac{2\pi}{T}k\lambda} \end{aligned} \quad (2.17)$$

where

$$R_k = \int_0^{T_0} r(t) e^{j\frac{2\pi}{T}kt} dt \quad (2.18)$$

So the test of Equation (2.6) becomes

$$\int_{-\infty}^{\infty} \exp\left\{\frac{2}{N_0} \sum_{k=-\infty}^{\infty} v_k R_k e^{-j\frac{2\pi}{T}k\lambda}\right\} f_{\Lambda}(\lambda) d\lambda \underset{H_0}{\overset{H_1}{>}} \eta \exp\{E/N_0\} \quad (2.19)$$

$$\frac{L_1(\underline{r})}{L_0(\underline{r})} = \int_{-\infty}^{\infty} \exp\left\{\frac{2}{N_0} \int_0^{T_0} r(t)v(t-\lambda)dt\right\} \cdot \exp\left\{-\frac{1}{N_0} \int_0^{T_0} v^2(t-\lambda)dt\right\} f_{\Lambda}(\lambda) d\lambda \quad \begin{matrix} H_1 \\ > \\ < \\ H_0 \end{matrix} \eta \quad (2.11)$$

Since $v(t)$ is T -periodic, it can be expressed in terms of an exponential Fourier series, namely

$$v(t) = \sum_{k=-\infty}^{\infty} v_k e^{j\frac{2\pi}{T}kt} \quad (2.12)$$

where

$$v_k = \frac{1}{T} \int_{-T/2}^{T/2} v(t) e^{-j\frac{2\pi}{T}kt} dt \quad \text{for all } k \quad (2.13)$$

Using the Fourier series expansion, we have

$$\int_0^{T_0} v^2(t-\lambda)dt = \sum_{k=-\infty}^{\infty} \sum_{\ell=-\infty}^{\infty} v_k v_{\ell} e^{-j\frac{2\pi}{T}(k+\ell)\lambda} \int_0^{T_0} e^{j\frac{2\pi}{T}(k+\ell)t} dt \quad (2.14)$$

However note that

$$\int_0^{T_0} e^{j\frac{2\pi}{T}(k+\ell)t} dt = \begin{cases} T_0 & \text{if } \ell = -k \\ 0 & \text{otherwise} \end{cases} \quad (2.15)$$

The likelihood ratio test is therefore

$$\frac{L_1(\underline{r})}{L_0(\underline{r})} \begin{matrix} > \\ < \end{matrix} \begin{matrix} H_1 \\ H_0 \end{matrix} \quad n \quad (2.6)$$

where

$$n = \frac{P\{H_0\} C_{10} - C_{00}}{P\{H_1\} C_{01} - C_{11}} \quad (2.7)$$

and

$$P\{H_i\} \quad i = 1, 0 \quad (2.8)$$

are the prior probabilities of occurrence of hypotheses H_i ,

and

$$C_{ij} \quad i, j = 0, 1 \quad (2.9)$$

are the costs associated with making decisions about hypotheses H_i . For a minimum probability of error receiver

$$C_{ij} = \begin{cases} 1 & i \neq j \\ 0 & i = j \end{cases} \quad (2.10)$$

Taking advantage of some simplifications in writing the LR, it is simple to show that the LR becomes

likelihood ratio (LR), with a threshold η and decide in favor of hypothesis H_1 if LR is greater than η , or in favor of H_0 if LR is less than η .

Due to the random variable λ , $v(t-\lambda)$ itself is a random process. If we condition on λ , i.e., we assume some fixed value of λ , then $v(t-\lambda)$ is completely known. However, the observed signal $r(t)$, conditioned on λ , because of the noise $n(t)$, is a Gaussian random process. In other words conditioning on λ , under either hypothesis, $r(t)$ is Gaussian so that the likelihood functions can be expressed in closed form and are given by [Ref. 4]

$$L_0(\underline{r}) = F \exp\left\{-\frac{1}{N_0} \int_0^{T_0} r^2(t) dt\right\} \quad (2.3)$$

and

$$L_1(\underline{r}|\lambda) = F \exp\left\{-\frac{1}{N_0} \int_0^{T_0} [r(t)-v(t-\lambda)]^2 dt\right\} \quad (2.4)$$

The constant F is of no consequence here as it will cancel once the LR, namely $L_1(\underline{r})/L_0(\underline{r})$ is evaluated. Observe that

$$L_1(\underline{r}) = \int_{-\infty}^{\infty} L_1(\underline{r}|\lambda) f_{\Lambda}(\lambda) d\lambda \quad (2.5)$$

C. COMPUTATION OF THE LIKELIHOOD RATIO

In this section, principles of statistical communication theory are applied to the derivation of a decision rule which will lead to the design of a receiver that optimally detects (with minimum probability of error, P_e) a periodic signal with random time delay, in the presence of additive white Gaussian noise (WGN) under the assumption of low signal to noise ratio conditions.

We start the problem by considering two hypotheses H_1 and H_0 such that during the observation interval $(0, T_0)$, under hypothesis H_1 , we assume that the periodic signal with unknown time delay is present and under the second hypothesis, i.e., H_0 , there is no signal present. In both cases, the effect of the WGN must be considered. Thus symbolically,

$$\left. \begin{array}{l} H_1: r(t) = v(t-\lambda) + n(t) \\ H_0: r(t) = n(t) \end{array} \right\} \quad 0 \leq t \leq T_0 \quad (2.2)$$

where

$r(t)$ = the signal at the front end of the receiver;

$v(t)$ = the T -periodic deterministic signal with λ a random variable modeling the unknown time delay of the waveform; and

$n(t)$ = a sample function of a white Gaussian process with zero mean and two-sided power spectral density level $N_0/2$ watts/Hz.

In order to satisfy the minimum probability of error criterion, the optimum decision rule is obtained by comparing the

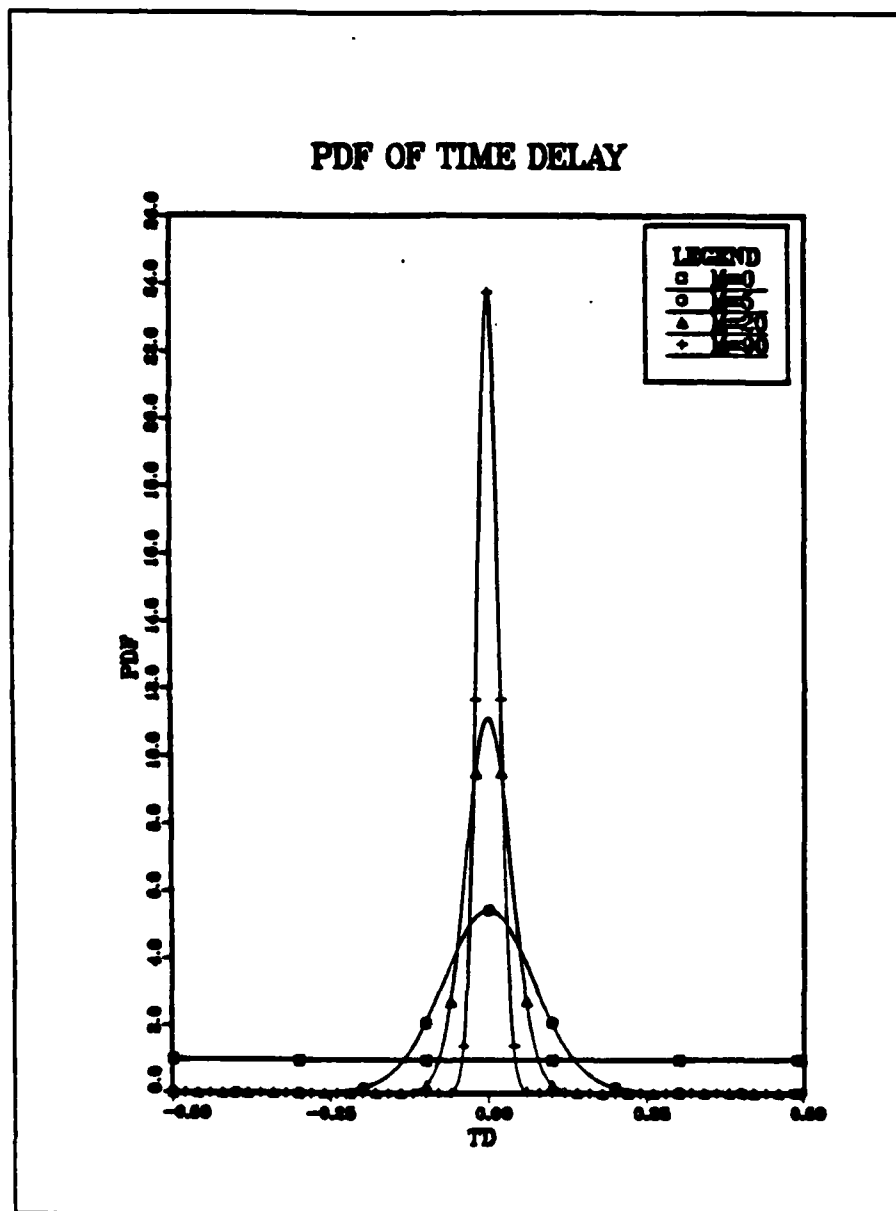


Figure 2.1 PDF of Time Delay

B. PROBABILITY DENSITY FUNCTION OF λ

The type of random signal parameter dealt with in this thesis is the phase or time delay of an arbitrary periodic waveform of period T . Generally, the period T of the signal is very much shorter than the time duration T_0 of the signal and therefore it is extremely difficult to predict the time delay at the receiver of such a signal. In such cases it is reasonable to model the time delay ' λ ', as random variable having some density function that reflects the degree of uncertainty that exists about λ .

A useful p.d.f. for the time delay [Ref. 3] is given by

$$f_{\Lambda}(\lambda; m) = \frac{e^{m \cos \frac{2\pi\lambda}{T}}}{T I_0(m)} \quad \begin{array}{l} \lambda \leq |T/2| \\ 0 \leq m \leq \infty \end{array} \quad (2.1)$$

where the independent parameter ' m ' determines the degree of uncertainty about the time delay λ , and $I_0(m)$ is a modified Bessel function of the first kind of order zero.

For $m = 0$, we see that $f_{\Lambda}(\lambda) = \frac{1}{T}$ for $\lambda \leq |T/2|$, so that λ is uniformly distributed over the period T . As m increases, the uncertainty of the random variable λ decreases and the p.d.f. approaches the shape of a normal density. As $m \rightarrow \infty$, $f_{\Lambda}(\lambda)$ tends to an impulse so that the time delay uncertainty tends to zero and the modeled random waveform approaches that of a deterministic or completely known signal. The shape of the p.d.f. as a function of m is shown in Fig. 2.1.

The derivation of the mean and variance of this density function is presented in Appendix A.

II. NONCOHERENT RECEIVER ANALYSIS

A. BASIC CONCEPT

Detection of arbitrary periodic signals with random time delay is a problem of significant importance in radar and communications, which has not received a great deal of attention in the past. The most relevant documentation related to this problem appears in the radar literature, where the problem is formulated as noncoherent detection of a radio frequency sine wave burst in the presence of noise [Ref. 1].

In communication systems, signals are transmitted to a receiver via some medium connecting the transmitter to the receiver called the channel. Transmitted signals undergo distortion in the channel as well as in the receiver itself. In many cases this distortion is caused by physical processes which, because of their complexity must be modeled via statistical means, i.e., random variables and/or processes. As previously pointed out in the receiver itself, noise is unavoidably added to the signals to cause further distortion and uncertainty. It is often found in practice, however, that the uncertainty created by the noise in a receiver results in the introduction of signal uncertainties, modeled as random processes having known waveshapes but random parameters such as random amplitudes, frequencies and/or phases. The problem of detecting signals of random time delay has been partially considered in Ref. 2.

have been carried out, and wherever possible, comparisons are made with optimum systems operating in similar environments.

The results of Chapters II and III involving receiver P_e are analyzed and interpreted via the use of tables and graphs in Chapter IV.

The fifth and final chapter presents some general conclusions to be derived from the work carried out in preparation of this thesis, and some suggestions for future analysis in this general topic area are given.

detect an arbitrarily shaped periodic waveform with random time delay, is carried out. The random time delay is assumed to have some known probability density function (p.d.f.). Two types of p.d.f.'s are assumed for the random time delay λ . Namely, a uniform p.d.f. and a (parameter varying) non-uniform p.d.f. have been considered, and their effect on the receiver probability of error (P_e) has been studied.

The design of optimum (in minimum P_e sense) receivers is based on the likelihood ratio and the assumption of low signal-to-noise ratio (SNR) operations. The design of suboptimum receivers is based on heuristic approaches that intuitively yield reasonably good performance.

Chapter II of this thesis presents statistical communication theoretic principles that have been applied to the analysis, design, and performance evaluation of noncoherent receivers. Approximations are made that lead to a decision rule or equivalently a receiver structure. A justification and meaning of such approximations is presented in Appendix B. It must be pointed out, that at high SNR, most receivers designed strictly from heuristic considerations perform adequately. At low SNR however, the receiver design must be optimum so as to not further degrade marginal operating conditions. Chapter II addresses this issue.

Chapter III is devoted to the analysis and design of suboptimum receivers where simple (heuristic) techniques have been applied to the design process. Performance evaluations

$$\begin{aligned}
\text{Var}\{\ell|H_1, \lambda\} &= E\{[(\ell|H_1, \lambda) - E\{\ell|H_1, \lambda\}]^2\} \\
&= E\left\{\left[V_0 \int_0^{T_0} [v(t-\lambda) + n(t)] dt - V_0 \int_0^{T_0} v(t-\lambda) dt\right]^2\right\} \\
&= V_0^2 \int_0^{T_0} \int_0^{T_0} E\{n(t)n(\tau)\} dt d\tau = \frac{N_0}{2} V_0^2 T_0 \\
&= \text{Var}\{\ell|H_0\} \triangleq \sigma_\ell^2 \tag{2.34}
\end{aligned}$$

Equation (2.33) shows that the conditional mean m_1 is independent of λ and Equation (2.34) also shows that the conditional variance of ℓ is independent of λ .

Hence

$$f_L(\ell|H_1, \lambda) = f_L(\ell|H_1) = \frac{1}{\sqrt{2\pi}\sigma_\ell} \exp\left\{-\frac{(\ell-m_1)^2}{2\sigma_\ell^2}\right\} \tag{2.35}$$

Also, from Equations (2.32) and (2.34)

$$f_L(\ell|H_0) = \frac{1}{\sqrt{2\pi}\sigma_\ell} \exp\left\{-\frac{\ell^2}{2\sigma_\ell^2}\right\} \tag{2.36}$$

The p.d.f.'s of Equations (2.35) and (2.36) are plotted in Fig. 2.3.

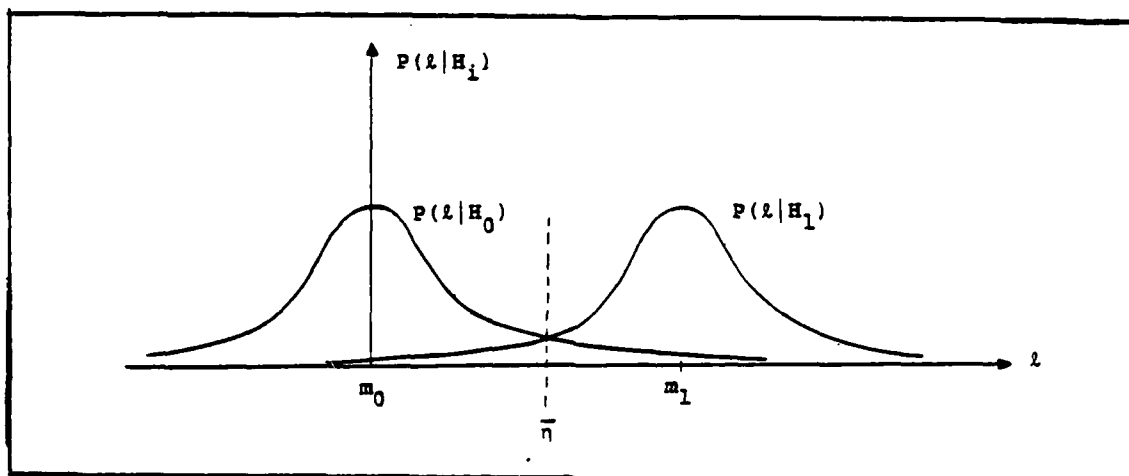


Fig. 2.3 Probability Density Function of l

From Equations (2.35) and (2.36) and Fig. 2.3, it is clear that the two p.d.f.'s are completely identical with different means. In order to have minimum probability of error, the threshold \bar{n} should be the point where the two p.d.f.'s intersect. That is,

$$\bar{n} = \frac{m_1 + m_0}{2} = \frac{V_0^2 T_0}{2} \quad (2.37)$$

This threshold differs from that given by Equation (2.24). We must however keep in mind that the results were obtained by approximations on the LR test of Equation (2.19).

Receiver probability of error P_e , is thus given by

$$P_e = P\{H_0\}P_F + P\{H_1\}P_M \quad (2.38)$$

where

P_F = Probability of false alarm;

P_M = Probability of miss; and

$P\{H_i\}$, $i = 0, 1$ are the prior probabilities.

Since we have assumed equal prior probabilities, P_e becomes

$$\begin{aligned}
 P_e &= \frac{1}{2} \int_{\eta_*}^{\infty} \frac{1}{\sqrt{2\pi}\sigma_\ell} e^{-\ell^2/2\sigma_\ell^2} d\ell + \frac{1}{2} \int_{-\infty}^{\eta_*} \frac{1}{\sqrt{2\pi}\sigma_\ell} e^{-(\ell-m_1)^2/2\sigma_\ell^2} d\ell \\
 &= \frac{1}{2} \int_{\eta_*/\sigma_\ell}^{\infty} \frac{1}{\sqrt{2\pi}} e^{-x^2/2} dx + \frac{1}{2} \int_{-\infty}^{(\eta_*-m_1)/\sigma_\ell} \frac{1}{\sqrt{2\pi}} e^{-y^2/2} dy \\
 &= \frac{1}{2} [\text{erfc}_* \left(\frac{\eta_*}{\sigma_\ell} \right) + \text{erf}_* \left(\frac{\eta_*-m_1}{\sigma_\ell} \right)] \quad (2.39)
 \end{aligned}$$

From Equations (2.24), (2.33) and (2.34), we get

$$P_e = \frac{1}{2} \left\{ \text{erfc}_* \left[\frac{e^{E/N_0} - 1}{\sqrt{\frac{2V_0^2 T_0}{N_0}}} \right] + \text{erf}_* \left[\frac{e^{E/N_0} - 1}{\sqrt{\frac{2V_0^2 T_0}{N_0}}} - \sqrt{\frac{2V_0^2 T_0}{N_0}} \right] \right\} \quad (2.40)$$

Observe that if $v(t)$ has a very strong d.c. component in comparison to its harmonics, then $V_0^2 T_0 / N_0$ is approximately equal to the SNR defined as E/N_0 . Then Equation (2.40) becomes a function of SNR only. Otherwise, it is a function of both the SNR and the $V_0^2 T_0 / N_0$ ratio.

2. Nonuniform p.d.f.

For this case, the p.d.f. of λ as given by Equation (2.1) is

$$f_{\Lambda}(\lambda) = \frac{e^{m \cos \frac{2\pi\lambda}{T}}}{T I_0(m)} \quad \lambda \leq |T/2|, \quad 0 \leq m \leq \infty$$

It is known that [Ref. 5]

$$\begin{aligned} e^{m \cos \theta} &= I_0(m) + 2 \sum_{p=1}^{\infty} I_p(m) \cos p\theta \\ &= \sum_{p=-\infty}^{\infty} I_p(m) \cos p\theta \end{aligned} \quad (2.41)$$

since

$$I_p(\cdot) = I_{-p}(\cdot)$$

Therefore, Equation (2.1) becomes

$$f_{\Lambda}(\lambda) = \frac{\sum_{p=-\infty}^{\infty} I_p(m) \cos p \frac{2\pi\lambda}{T}}{T I_0(m)} \quad (2.42)$$

From Equation (2.23) we have the test

$$\sum_{k=-\infty}^{\infty} V_k R_k \int_{-\infty}^{\infty} f_{\Lambda}(\lambda) e^{-j \frac{2\pi k}{T} \lambda} d\lambda \begin{matrix} H_1 \\ > \\ < \\ H_0 \end{matrix} \eta_*$$

or equivalently

$$\sum_{k=-\infty}^{\infty} V_k R_k F_{\Lambda}\left(\frac{2\pi k}{T}\right) \begin{matrix} H_1 \\ > \\ < \\ H_0 \end{matrix} \eta_* \quad (2.43)$$

where

$$F_{\Lambda}\left(\frac{2\pi k}{T}\right) = \int_{-\infty}^{\infty} f_{\Lambda}(\lambda) e^{-j\frac{2\pi k}{T}\lambda} d\lambda \quad (2.44)$$

Substituting Equation (2.42) into (2.44), we get

$$\begin{aligned} F_{\Lambda}\left(\frac{2\pi k}{T}\right) &= \frac{1}{TI_0(m)} \sum_{p=-\infty}^{\infty} I_p(m) \int_{-T/2}^{T/2} \cos p\frac{2\pi\lambda}{T} e^{-j\frac{2\pi k}{T}\lambda} d\lambda \\ &= \frac{1}{2TI_0(m)} \sum_{p=-\infty}^{\infty} I_p(m) \left[\int_{-T/2}^{T/2} e^{j\frac{2\pi}{T}(p-k)\lambda} d\lambda \right. \\ &\quad \left. + \int_{-T/2}^{T/2} e^{-j\frac{2\pi}{T}(p+k)\lambda} d\lambda \right] \end{aligned} \quad (2.45)$$

Note that both integrals in Equation (2.45) are zero unless $p = \pm k$. For $p = k$, first integral in brackets is T , and the second integral becomes zero. For $p = -k$, the first integral is zero but the second integral is T .

Therefore

$$F_{\Lambda}\left(\frac{2\pi k}{T}\right) = \frac{I_k(m)}{I_0(m)}, \quad (2.46)$$

since

$$I_{-k}(\cdot) = I_k(\cdot).$$

Hence the test of Equation (2.43) becomes

$$\frac{1}{I_0(m)} \sum_{k=-\infty}^{\infty} V_k R_k I_k(m) \begin{matrix} H_1 \\ > \\ < \\ H_0 \end{matrix} \eta_* \quad (2.47)$$

The test can be simplified further by letting

$$\begin{aligned} g &= \frac{1}{I_0(m)} \sum_{k=-\infty}^{\infty} V_k R_k I_k(m) \\ &= \frac{1}{I_0(m)} \left\{ V_0 I_0(m) \int_0^{T_0} r(t) dt + \sum_{k=1}^{\infty} V_k I_k(m) \int_0^{T_0} r(t) e^{j\frac{2\pi k}{T}t} dt \right. \\ &\quad \left. + \sum_{k=1}^{\infty} V_k I_k(m) \int_0^{T_0} r(t) e^{j\frac{2\pi k}{T}t} dt \right\} \\ &= \frac{1}{I_0(m)} \left\{ V_0 I_0(m) \int_0^{T_0} r(t) dt \right. \\ &\quad \left. + 2 \sum_{k=1}^{\infty} |V_k| I_k(m) \int_0^{T_0} r(t) \cos\left(\frac{2\pi k}{T}t + \alpha_k\right) dt \right\} \quad (2.48) \end{aligned}$$

where

$$v_{\pm k} = |v_k| e^{\pm j\alpha_k} \quad (2.49)$$

Finally the test becomes

$$v_0 \int_0^{T_0} r(t) dt + \frac{2}{I_0(m)} \sum_{k=1}^{\infty} |v_k| I_k(m) \int_0^{T_0} r(t) \cos\left(\frac{2\pi k}{T} t + \alpha_k\right) dt \begin{matrix} > \\ < \end{matrix} \begin{matrix} H_1 \\ H_0 \end{matrix} \eta_* \quad (2.50)$$

and the receiver may be implemented as shown in Fig. 2.4.

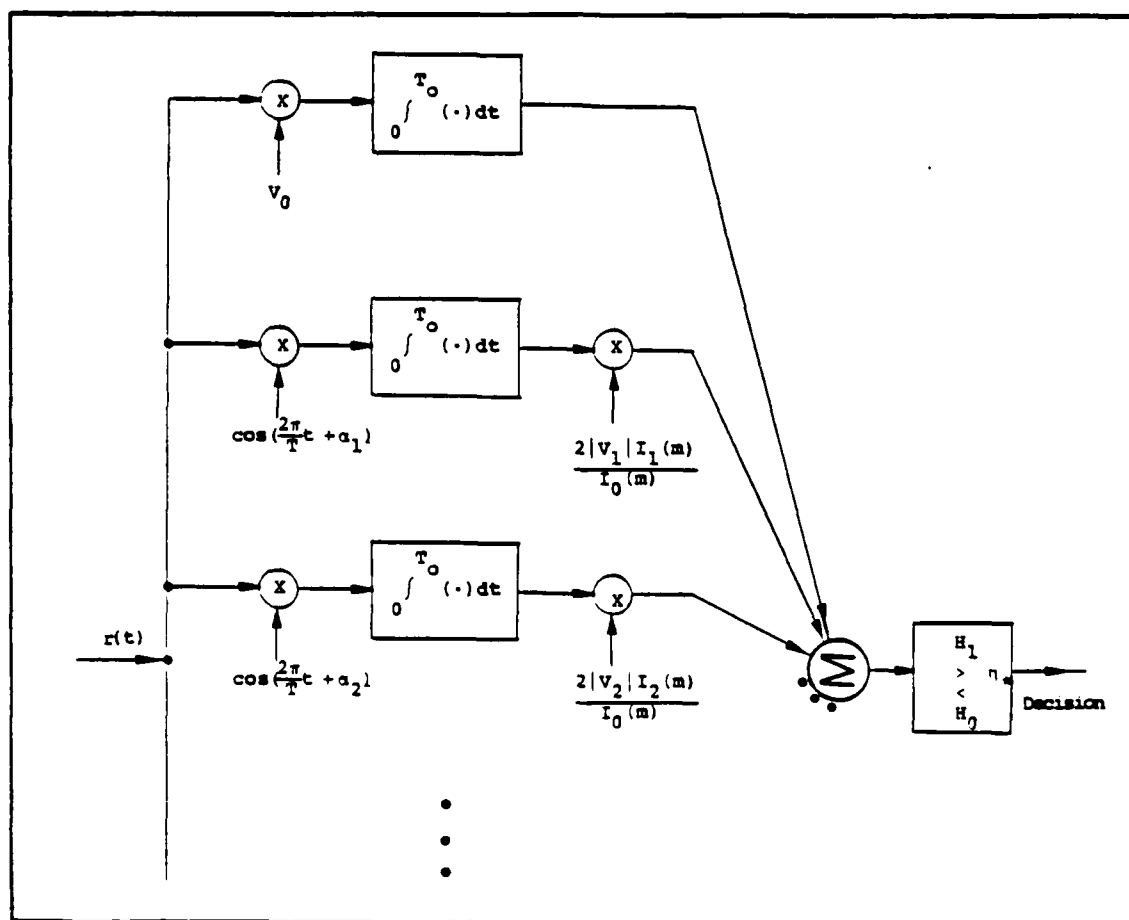


Figure 2.4 Noncoherent Receiver (Nonuniform p.d.f., 2 Term Approximation)

Notice that this receiver can operate on signals both with and without d.c. component. When a signal has zero d.c. term, the receiver of Fig. 2.4 can be simplified by eliminating the uppermost branch.

The performance of this receiver is obtained by using the fact that conditioned on λ , under either hypothesis, g is a Gaussian random variable with

$$E\{g|H_0\} = 0 \quad (2.51)$$

and

$$\begin{aligned} E\{g|H_1, \lambda\} &= E\left\{\frac{1}{I_0(m)} \sum_{k=-\infty}^{\infty} V_k I_k(m) \int_0^{T_0} v(t-\lambda) e^{j\frac{2\pi k}{T}t} dt\right\} \\ &= \frac{1}{I_0(m)} \sum_{k=-\infty}^{\infty} \sum_{\ell=-\infty}^{\infty} V_k V_{\ell} I_k(m) e^{-j\frac{2\pi \ell}{T}\lambda} \int_0^{T_0} e^{j\frac{2\pi}{T}(\ell+k)t} dt \end{aligned} \quad (2.52)$$

The integral of Equation (2.52) has been analyzed in Equation (2.15). Therefore

$$E\{g|H_1, \lambda\} = \frac{T_0}{I_0(m)} \sum_{k=-\infty}^{\infty} |V_k|^2 I_k(m) e^{j\frac{2\pi k}{T}\lambda} \triangleq h(\lambda) \quad (2.53)$$

Furthermore,

$$\begin{aligned}
\text{Var}\{g|H_1, \lambda\} &= E\left\{\left(\frac{1}{I_0(m)} \sum_{k=-\infty}^{\infty} V_k I_k(m) \int_0^{T_0} [v(t-\lambda) + n(t)] e^{j\frac{2\pi k}{T}t} dt \right.\right. \\
&\quad \left.\left. - \frac{1}{I_0(m)} \sum_{k=-\infty}^{\infty} V_k I_k(m) \int_0^{T_0} v(t-\lambda) e^{j\frac{2\pi k}{T}t} dt \right)^2\right\} \\
&= E\left\{\left(\frac{1}{I_0(m)} \sum_{k=-\infty}^{\infty} V_k I_k(m) \int_0^{T_0} n(t) e^{j\frac{2\pi k}{T}t} dt \right)^2\right\} \\
&= \frac{1}{I_0^2(m)} \sum_{k=-\infty}^{\infty} \sum_{\ell=-\infty}^{\infty} V_k V_{\ell} I_k(m) I_{\ell}(m) \int_0^{T_0} \int_0^{T_0} E\{n(t)n(\tau)\} \\
&\quad \cdot e^{j\frac{2\pi k}{T}t} e^{j\frac{2\pi \ell}{T}\tau} dt d\tau \\
&= \frac{1}{I_0^2(m)} \frac{N_0}{2} \sum_{k=-\infty}^{\infty} \sum_{\ell=-\infty}^{\infty} V_k V_{\ell} I_k(m) I_{\ell}(m) \int_0^{T_0} e^{j\frac{2\pi}{T}(k+\ell)t} dt \\
&= \frac{T_0 N_0}{2 I_0^2(m)} \sum_{k=-\infty}^{\infty} |V_k|^2 I_k^2(m) \\
&= \text{Var}\{g|H_1\} = \text{Var}\{g|H_0\} \triangleq \sigma_g^2 \quad (2.54)
\end{aligned}$$

With $p = P\{H_0\}$ and $1-p = P\{H_1\}$, we have an expression for the conditional P_e given by

$$\begin{aligned}
P_e(\lambda) &= p \int_{\eta_*}^{\infty} f_G(g|H_0) dg + (1-p) \int_{-\infty}^{\eta_*} f_G(g|H_1, \lambda) dg \\
&= p \int_{\eta_*}^{\infty} \frac{1}{\sqrt{2\pi}\sigma_g} e^{-g^2/2\sigma_g^2} dg + (1-p) \int_{-\infty}^{\eta_*} \frac{1}{\sqrt{2\pi}\sigma_g} e^{-(g-h(\lambda))^2/2\sigma_g^2} dg \\
&= p \operatorname{erfc}_*\left(\frac{\eta_*}{\sigma_g}\right) + (1-p) \operatorname{erf}_*\left(\frac{\eta_*-h(\lambda)}{\sigma_g}\right) \quad (2.55)
\end{aligned}$$

where η_* , $h(\lambda)$ and σ_g are given by Equations (2.24), (2.53) and (2.54), respectively.

The actual receiver P_e is obtained by integrating $P_e(\lambda)$ over the p.d.f. of λ , resulting in

$$P_e = p \operatorname{erfc}_*\left(\frac{\eta_*}{\sigma_g}\right) + (1-p) \int_{-\infty}^{\infty} f_{\Lambda}(\lambda) \operatorname{erf}_*\left(\frac{\eta_*-h(\lambda)}{\sigma_g}\right) d\lambda \quad (2.56)$$

Observe that

$$\begin{aligned}
\frac{\eta_*}{\sigma_g} &= \left[\frac{\frac{N_o^2}{4} (e^{E/N_o} - 1)^2}{\frac{N_o T_o}{2 I_0^2(m)} \sum_{k=-\infty}^{\infty} |v_k|^2 I_k^2(m)} \right]^{1/2} \\
&= \frac{e^{E/N_o} - 1}{\left[\frac{2E}{N_o} \sum_{k=-\infty}^{\infty} |v_k|^2 I_k^2(m) / I_0^2(m) \sum_{\ell=-\infty}^{\infty} |v_{\ell}|^2 \right]^{1/2}} \quad (2.57)
\end{aligned}$$

Also

$$\frac{h(\lambda)}{\sigma_g} = \left[\frac{\frac{T_0^2}{I_0^2(m)} \left(\sum_{k=-\infty}^{\infty} |v_k|^2 I_k(m) e^{j \frac{2\pi k \lambda}{T}} \right)^2}{\frac{N_0 T_0}{2 I_0^2(m)} \sum_{k=-\infty}^{\infty} |v_k|^2 I_k^2(m)} \right]^{1/2}$$

$$= \frac{\frac{2E}{N_0} \sum_{k=-\infty}^{\infty} |v_k|^2 I_k(m) e^{j \frac{2\pi k \lambda}{T}} / I_0(m) \sum_{\ell=-\infty}^{\infty} |v_\ell|^2}{\left[\frac{2E}{N_0} \sum_{k=-\infty}^{\infty} |v_k|^2 I_k^2(m) / I_0^2(m) \sum_{\ell=-\infty}^{\infty} |v_\ell|^2 \right]^{1/2}} \quad (2.58)$$

E. THREE TERM APPROXIMATION

Whenever Equation (2.20) is not satisfied to the degree that Equation (2.21) is valid, it is possible to proceed with the analysis beyond Equation (2.19), if in Equation (2.19) we expand the exponential term and approximate it with three terms. Since

$$\exp\{x\} \approx 1 + x + \frac{x^2}{2!}, \quad \text{if } x \ll 1 \quad (2.59)$$

in order to have the approximation error not exceed 10%, we must have $x \leq 0.79$. Using the three term approximation of Equation (2.59) and applying it to Equation (2.19), the test then becomes

$$\int_{-\infty}^{\infty} \left[1 + \frac{2}{N_0} \sum_{k=-\infty}^{\infty} v_k R_k e^{-j \frac{2\pi k \lambda}{T}} + \frac{1}{2} \left(\frac{2}{N_0} \sum_{k=-\infty}^{\infty} v_k R_k e^{-j \frac{2\pi k \lambda}{T}} \right)^2 \right] f_{\Lambda}(\lambda) d\lambda \begin{matrix} H_1 \\ > \\ < \\ H_0 \end{matrix} n e^{E/N_0} \quad (2.60)$$

or equivalently

$$\frac{2}{N_0} \sum_{k=-\infty}^{\infty} V_k R_k \int_{-\infty}^{\infty} f_{\Lambda}(\lambda) e^{-j \frac{2\pi k \lambda}{T}} d\lambda + \frac{1}{2} \int_{-\infty}^{\infty} \left(\frac{2}{N_0} \sum_{k=-\infty}^{\infty} V_k R_k e^{-j \frac{2\pi k \lambda}{T}} \right)^2 \cdot f_{\Lambda}(\lambda) d\lambda \begin{matrix} H_1 \\ > \\ < \\ H_0 \end{matrix} \gamma \quad (2.61)$$

where

$$\gamma = (ne^{E/N_0} - 1) \quad (2.62)$$

Here again, two cases must be considered:

1. Uniform p.d.f. on λ
 2. Nonuniform p.d.f. on λ
1. Uniform p.d.f.

For this case the first term on the left hand side (L.H.S.) of the inequality in Equation (2.61) has already been analyzed in Equations (2.26) through (2.28). This first term is just $V_0 R_0$. The second term of Equation (2.61), i.e.,

$$\frac{1}{2} \int_{-\infty}^{\infty} \left(\frac{2}{N_0} \sum_{k=-\infty}^{\infty} V_k R_k e^{-j \frac{2\pi k \lambda}{T}} \right)^2 f_{\Lambda}(\lambda) d\lambda$$

becomes (with the aid of Equation (2.15))

$$\frac{1}{2T} \cdot \frac{4}{N_0^2} \sum_{k=-\infty}^{\infty} \sum_{\ell=-\infty}^{\infty} V_k R_k V_{\ell} R_{\ell} \int_0^T e^{-j \frac{2\pi}{T} (k+\ell) \lambda} d\lambda = \frac{2}{N_0^2} \sum_{k=-\infty}^{\infty} |V_k|^2 |R_k|^2 \quad (2.63)$$

The test therefore becomes

$$\frac{V_0 R_0}{N_0} + \frac{1}{N_0^2} \sum_{k=-\infty}^{\infty} |V_k|^2 |R_k|^2 \underset{H_0}{\overset{H_1}{>}} \frac{\gamma}{2} \triangleq \gamma^* \quad (2.64)$$

or equivalently (using Equations (2.13) and (2.18))

$$\begin{aligned} \frac{V_0}{N_0} \int_0^{T_0} r(t) dt + \left[\frac{V_0}{N_0} \int_0^{T_0} r(t) dt \right]^2 \\ + 2 \sum_{k=1}^{\infty} \left[\frac{|V_k|}{N_0} \int_0^{T_0} r(t) \cos \frac{2\pi k}{T} t dt \right]^2 \underset{H_0}{\overset{H_1}{>}} \gamma^* \end{aligned} \quad (2.65)$$

This test leads to the receiver structure shown in Fig. 2.5.

Note that this receiver utilizes both the d.c. and non-d.c. components of the periodic signal. However, in practice there are many cases where the d.c. component of the signal is zero. For those cases, the test reduces to

$$\frac{2}{N_0} \sum_{k=1}^{\infty} |V_k|^2 |R_k|^2 \underset{H_0}{\overset{H_1}{>}} \gamma^* \quad (2.66)$$

and the corresponding receiver can be implemented by simply eliminating the upper most branch of the receiver in Fig. 2.5.

2. Nonuniform p.d.f.

Our starting point here is Equation (2.11), repeated here for convenience,

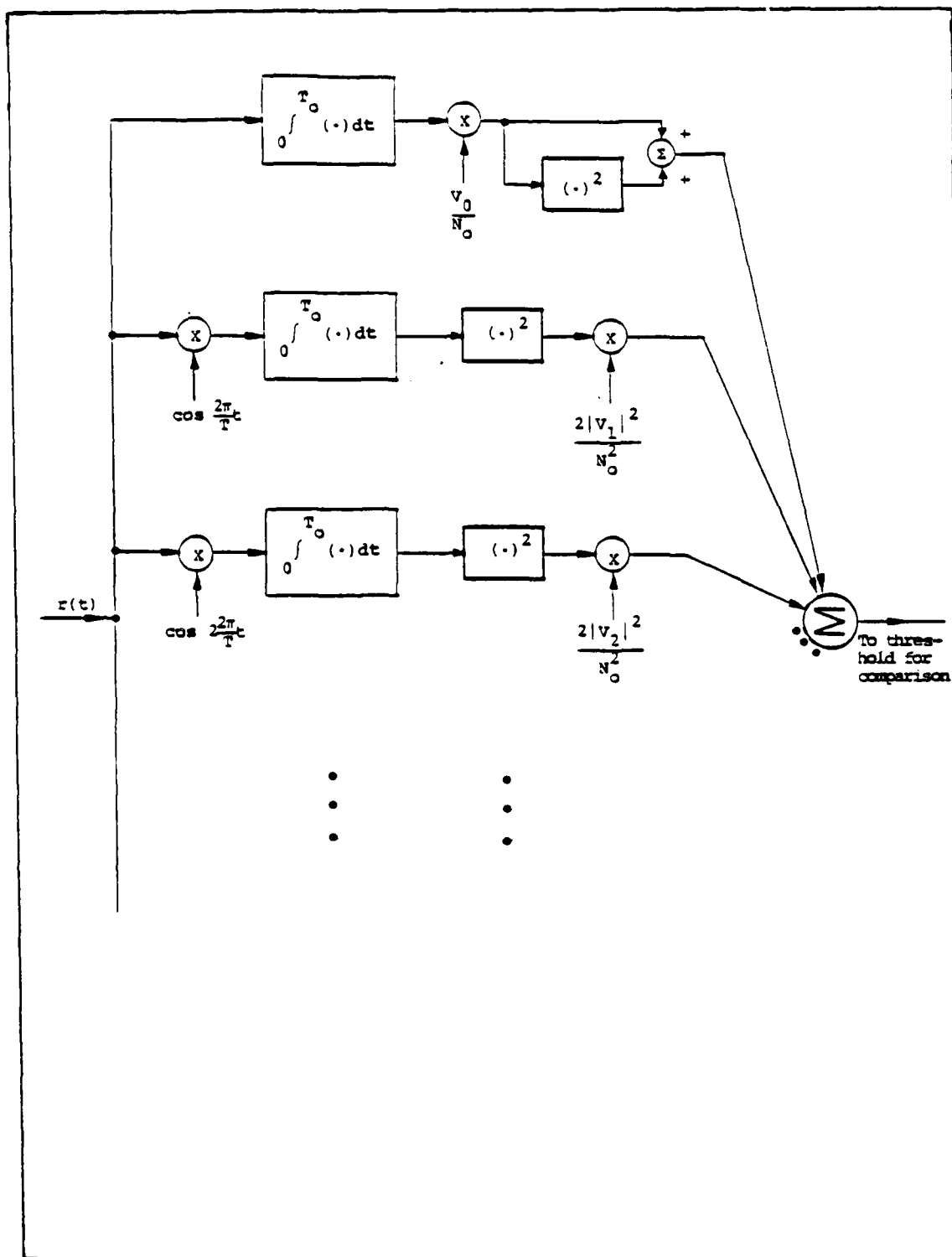


Fig. 2.5 Noncoherent Receiver (Uniform p.d.f., 3 Term Approximation)

where

$$\Lambda_{nm} \triangleq \int_0^{T_0} v(t - \frac{nT}{N}) v(t - \frac{mT}{N}) dt \quad (3.6)$$

are the signal discrete cross correlation terms. Thus,

$$E\{\ell | H_0\} = \sum_{n=1}^N E\{r_n | H_0\} = 0 \quad (3.7)$$

and

$$\begin{aligned} E\{\ell^2 | H_0\} &= E\left\{ \sum_{n=1}^N \sum_{m=1}^N r_n r_m | H_0 \right\} \\ &= \frac{N_0}{2} \sum_{n=1}^N \sum_{m=1}^N \Lambda_{nm} \triangleq \sigma_\ell^2 \end{aligned} \quad (3.8)$$

Now conditioned on both H_1 and λ , ℓ is also a Gaussian r.v. with

$$E\{r_n | H_1, \lambda\} = \int_0^{T_0} v(t - \lambda) v(t - \frac{nT}{N}) dt \triangleq \alpha_n(\lambda) \quad (3.9)$$

and

$$\ell = \sum_{n=1}^N \int_0^{T_0} r(t) v(t - \frac{nT}{N}) dt = \sum_{n=1}^N r_n \quad (3.1)$$

where

$$r_n \triangleq \int_0^{T_0} r(t) v(t - \frac{nT}{N}) dt \quad (3.2)$$

If we consider the two hypotheses, as done in Chapter II, namely

$$\left. \begin{array}{l} H_1: r(t) = v(t-\lambda) + n(t) \\ H_0: r(t) = n(t) \end{array} \right\} \quad 0 \leq t \leq T_0 \quad (3.3)$$

then conditioned on hypothesis H_0 , ℓ is a Gaussian random variable (r.v.) with

$$E\{r_n | H_0\} = 0 \quad (3.4)$$

since the noise is assumed to be zero mean, and

$$\begin{aligned} E\{r_n r_m | H_0\} &= E\left\{ \int_0^{T_0} n(t) v(t - \frac{nT}{N}) dt \int_0^{T_0} n(\tau) v(\tau - \frac{mT}{N}) d\tau \right\} \\ &= \frac{N_0}{2} \int_0^{T_0} v(t - \frac{nT}{N}) v(t - \frac{mT}{N}) dt = \frac{N_0}{2} \Lambda_{nm} \end{aligned} \quad (3.5)$$

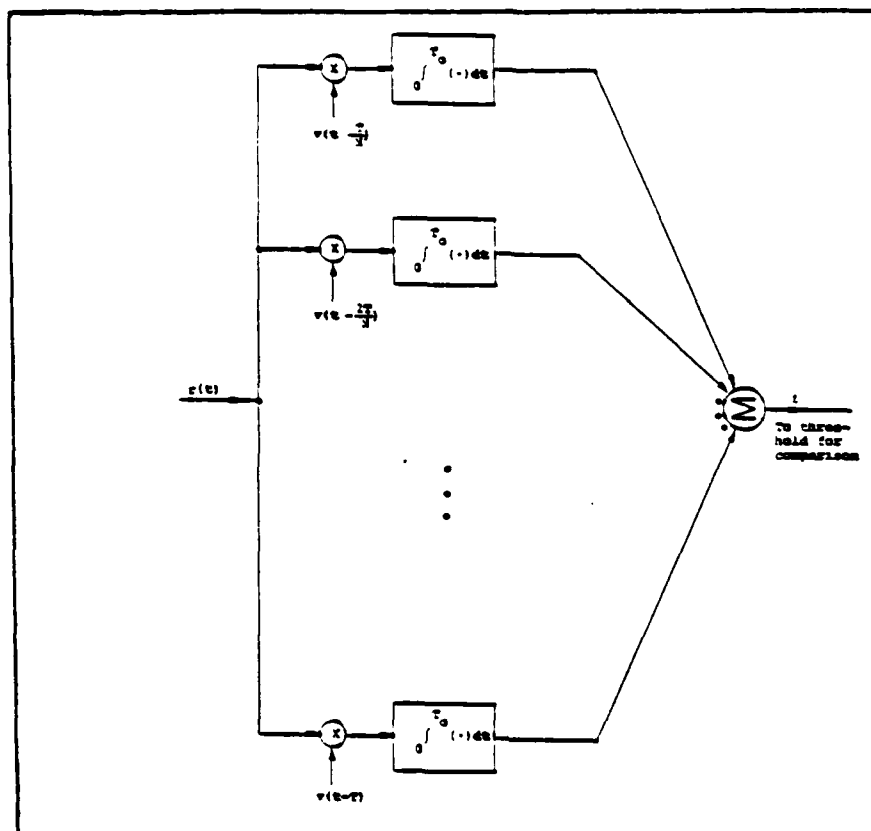


Fig. 3.1. N-Correlator Receiver

these conditions than when the correlators are fed by low level noise only. Thus, if ℓ is greater than a prescribed threshold, then the presence of a signal with a random time delay is declared; otherwise only the presence of noise is declared. Here we assume for convenience that the observation time T_0 is an integral multiple of T , the period of the signal $v(t)$. Observe furthermore that we are not required to assume low SNR conditions as done in Chapter II.

In order to analyze this receiver in more detail, observe that

III. ALTERNATIVE SUBOPTIMUM RECEIVERS

In the previous chapter, optimum detectors based on likelihood ratio tests were derived under conditions that are equivalent to low SNR conditions for signals having random time delay in the presence of additive white Gaussian noise. The tests derived gave rise to different receiver structures which, whenever possible, were analyzed in terms of their error probability performance. Both the receiver structures and their performance were seen to be a function of the uncertainty in the signal time delay or more precisely, a function of the p.d.f. of the signal time delay λ .

In this chapter, two suboptimum receivers are analyzed. The approach used here is different in the sense that receivers are derived via strictly heuristic means and their performances are then analyzed. These receivers are:

- A. N-correlator Receiver
- B. Estimator-correlator Receiver

A. N-CORRELATOR RECEIVER

This receiver is shown in Fig. 3.1. The idea is to correlate the received signal $r(t)$ with N delayed reference signals generated at the receiver. If a signal is present, presumably at least one correlator branch would produce a large output so that the sum ℓ could be guaranteed to be much larger under

Observe that Equation (2.90) (as well as Equations (2.57) and (2.58)) involve summations whose index runs from 1 to infinity. In practice, it is not possible to compute infinite sums. However, due to the fact that for all reasonable signals $v(t)$, the magnitude of the V_k coefficients gets smaller as k gets bigger, the infinite sum can be truncated without introducing significant computational error. Furthermore, terms involving the magnitude squared of these coefficients will tend to decay more rapidly allowing early truncation of the infinite sums.

G. DISCUSSION

In order to carry out the evaluation of Equation (2.90) to a reasonable degree of accuracy, the mathematical expression given by Equation (2.90) was evaluated by computer for fixed SNR values. Computation of P_e was carried out for a fixed value on the upper limit on the index k . Recomputation of P_e was carried out everytime this upper summation limit was incremented by 1. Recomputation of P_e was stopped after an incrementation of the upper limit in the sum terms did not yield an appreciably different value for P_e in comparison to the P_e value before incrementation.

The result of these evaluations has been presented in Chapter IV in the form of tables and graphs while P_e has been plotted as a function of SNR for different values of the parameter m . Recall that m specifies our relative prior knowledge about the signal's random time delay.

Hence Equation (2.57) becomes

$$\frac{\eta_{\star}}{\sigma_g} = \frac{(ne^{\frac{E}{N_0}} - 1)}{\left[\frac{4E/N_0 \sum_{k=1}^{\infty} |v_k|^2 I_k^2(m)}{A^2 I_0^2(m)} \right]} \quad (2.88)$$

and Equation (2.58) becomes

$$\frac{\eta_{\star} - h(\lambda)}{\sigma_g} = \frac{(ne^{\frac{E}{N_0}} - 1) - \left(\frac{4E/N_0}{I_0(m)A^2} \right) \left(\sum_{k=1}^{\infty} |v_k|^2 I_k^2(m) \cos \frac{2\pi k \lambda}{T} \right)}{\left[\frac{4E/N_0 \sum_{k=1}^{\infty} |v_k|^2 I_k^2(m)}{I_0^2(m)A^2} \right]} \quad (2.89)$$

Thus Equation (2.56) for the receiver probability of error becomes

$$P_e = p \operatorname{erfc} \star \left\{ \frac{(ne^{\frac{E}{N_0}} - 1)}{\left[\frac{4E/N_0 \sum_{k=1}^{\infty} |v_k|^2 I_k^2(m)}{I_0^2(m)A^2} \right]^{1/2}} \right\} \\ + (1-p) \int_0^T \operatorname{erf} \star \left\{ \frac{(ne^{\frac{E}{N_0}} - 1) - \left(\frac{4E/N_0}{I_0(m)A^2} \right) \left(\sum_{k=1}^{\infty} |v_k|^2 I_k^2(m) \cos \frac{2\pi k \lambda}{T} \right)}{\left[\frac{4E/N_0 \sum_{k=1}^{\infty} |v_k|^2 I_k^2(m)}{I_0^2(m)A^2} \right]^{1/2}} \right\} \\ \cdot \frac{e^{m \cos \frac{2\pi \lambda}{T}}}{T I_0(m)} d\lambda \quad (2.90)$$

Note that

$$\int_{-T/2}^{T/2} v^2(t) dt = A^2 T = T \sum_{k=-\infty}^{\infty} |v_k|^2 \quad (2.84)$$

which implies that

$$\sum_{k=-\infty}^{\infty} |v_k|^2 = A^2 \quad (2.85)$$

Furthermore

$$\sum_{k=-\infty}^{\infty} |v_k|^2 I_k(m) = |v_0|^2 I_0(m) + 2 \sum_{k=1}^{\infty} |v_k|^2 I_k(m) \quad (2.86)$$

so that

$$\begin{aligned} \sum_{k=-\infty}^{\infty} |v_k|^2 I_k(m) e^{-j \frac{2\pi k}{T} \lambda} &= |v_0|^2 I_0(m) \\ &+ 2 \sum_{k=1}^{\infty} |v_k|^2 I_k(m) \cos \frac{2\pi k}{T} \lambda \end{aligned} \quad (2.87)$$

since

$$|v_k| = |v_{-k}|; \quad I_k(m) = I_{-k}(m)$$

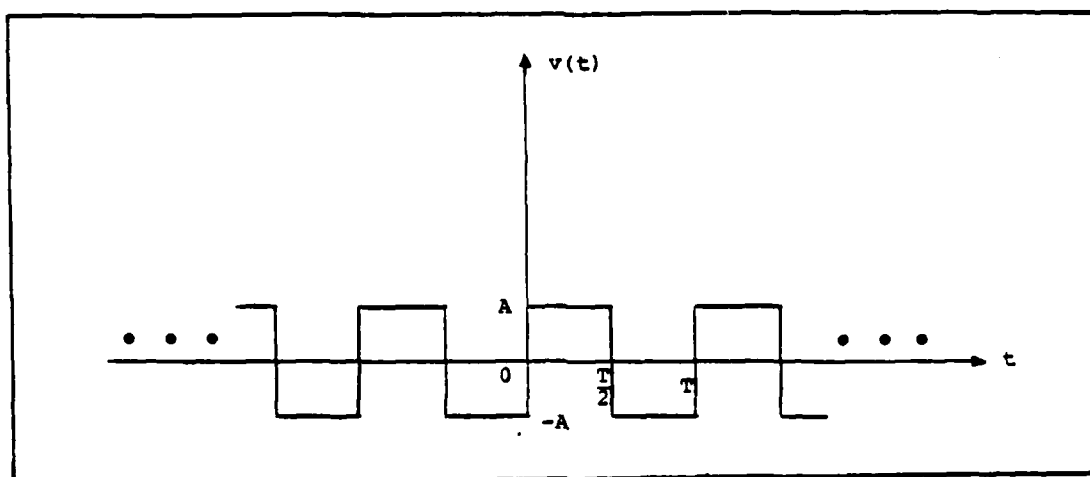


Fig. 2.7 Periodic Square Wave

The Fourier coefficients of $v(t)$ are

$$\begin{aligned}
 v_k &= \frac{1}{T} \left[\int_0^{T/2} A e^{-j\frac{2\pi k}{T}t} dt - \int_{T/2}^T A e^{-j\frac{2\pi k}{T}t} dt \right] \\
 &= \frac{j\pi k}{2} A e^{-j\pi k} \left[\frac{\sin \frac{\pi k}{2}}{\frac{\pi k}{2}} \right]^2 \quad (2.81)
 \end{aligned}$$

Observe that v_0 and all the even coefficients are zero, i.e.,

$$v_{2k} = 0 \quad \text{for all } k \quad (2.82)$$

and

$$\begin{aligned}
 v_{\pm k} &= j \frac{2A}{k\pi}, \quad |v_{\pm k}| = \frac{2A}{k\pi}, \quad |v_{\pm k}|^2 = \left(\frac{2A}{k\pi}\right)^2, \quad (2.83) \\
 &\quad k \text{ odd}
 \end{aligned}$$

$$\frac{\eta \star h(\lambda)}{\sigma_g} = \frac{(e^{E/N_o} - 1) - \left(\frac{2E}{N_o} \frac{I_1(m)}{I_0(m)} \cos \frac{2\pi\lambda}{T} \right)}{\frac{I_1(m)}{I_0(m)} (2E/N_o)^{1/2}} \quad (2.79)$$

Thus the expression for P_e becomes

$$P_e = p \operatorname{erfc} \star \left\{ \frac{(e^{E/N_o} - 1)}{\frac{I_1(m)}{I_0(m)} (2E/N_o)^{1/2}} \right\} + \frac{(1-p)}{T I_0(m)} \int_{-T/2}^{T/2} \operatorname{erf} \star \left\{ \frac{(e^{E/N_o} - 1) - \frac{2E}{N_o} \frac{I_1(m)}{I_0(m)} \cos \frac{2\pi\lambda}{T}}{\frac{I_1(m)}{I_0(m)} (2E/N_o)^{1/2}} \right\} e^{m \cos \frac{2\pi\lambda}{T}} d\lambda \quad (2.80)$$

Computation of Equation (2.80) can be carried out as a function of the SNR E/N_o , p and m . This has been carried out, and the results are presented graphically in Chapter IV. For the sake of computational simplicity, equal prior probabilities were assumed, i.e.,

$$p = 1-p = \frac{1}{2}$$

resulting in $\eta = 1$.

2. Square Wave

For the second case, let $v(t)$ be a periodic square wave as shown in Fig. 2.7.

1. Sine Wave
2. Square Wave

1. Sine Wave

For the first case let

$$\begin{aligned}
 v(t) &= A \cos \frac{2\pi}{T}t \\
 &= \frac{A}{2} e^{j\frac{2\pi}{T}t} + \frac{A}{2} e^{-j\frac{2\pi}{T}t}
 \end{aligned} \tag{2.75}$$

This periodic signal has only two discrete components. In other words, it can be represented in terms of its two Fourier coefficients, i.e.,

$$v_k = \begin{cases} \frac{A}{2} & k = \pm 1 \\ 0 & \text{otherwise} \end{cases} \tag{2.76}$$

Thus,

$$\sum_{k=-\infty}^{\infty} |v_k|^2 = \left(\frac{A}{2}\right)^2 + \left(\frac{A}{2}\right)^2 = \frac{A^2}{2} \tag{2.77}$$

and from Equations (2.57) and (2.58), we obtain

$$\frac{\eta_{\star}}{\sigma_g} = \frac{\frac{(e^{E/N_o} - 1)}{I_1(m)}}{I_0(m) (2E/N_o)^{1/2}} \tag{2.78}$$

$$\begin{aligned}
R_Y(t, \tau) &= \frac{1}{T} \sum_{k=-\infty}^{\infty} \sum_{\ell=-\infty}^{\infty} V_k V_{\ell} e^{j \frac{2\pi k}{T} t} e^{j \frac{2\pi \ell}{T} \tau} \int_{-T/2}^{T/2} e^{-j \frac{2\pi}{T} (k+\ell) \lambda} d\lambda \\
&= \sum_{k=-\infty}^{\infty} |V_k|^2 e^{j \frac{2\pi k}{T} (t-\tau)} \quad (2.74)
\end{aligned}$$

which is a function of $(t-\tau)$ only. This implies that for the uniform p.d.f. on λ , the impulse response of the filter turns out to be time invariant. That is, it depends only on the time difference $(t-\tau)$. Furthermore, $m_Y(t)$ being a constant can be eliminated from the upper branch of the receiver shown in Fig. 2.6.

F. ANALYSIS OF TWO SPECIFIC SIGNAL WAVESHAPES

It was pointed out earlier that the receiver derived using a two term approximation on the exponential appearing in Equation (2.19), is unable to discriminate between the signal present versus the signal absent case for signals having zero d.c. component when the random time delay obeys a uniform distribution. When the random time delay obeys a nonuniform p.d.f., a receiver was derived (see Fig. 2.4) that could detect the presence of signals having zero d.c. component.

In this section, assuming a nonuniform p.d.f. on λ , the receiver performance will be analyzed for two different signals which are found quite often in practice and that have a zero d.c. component. The two signals are

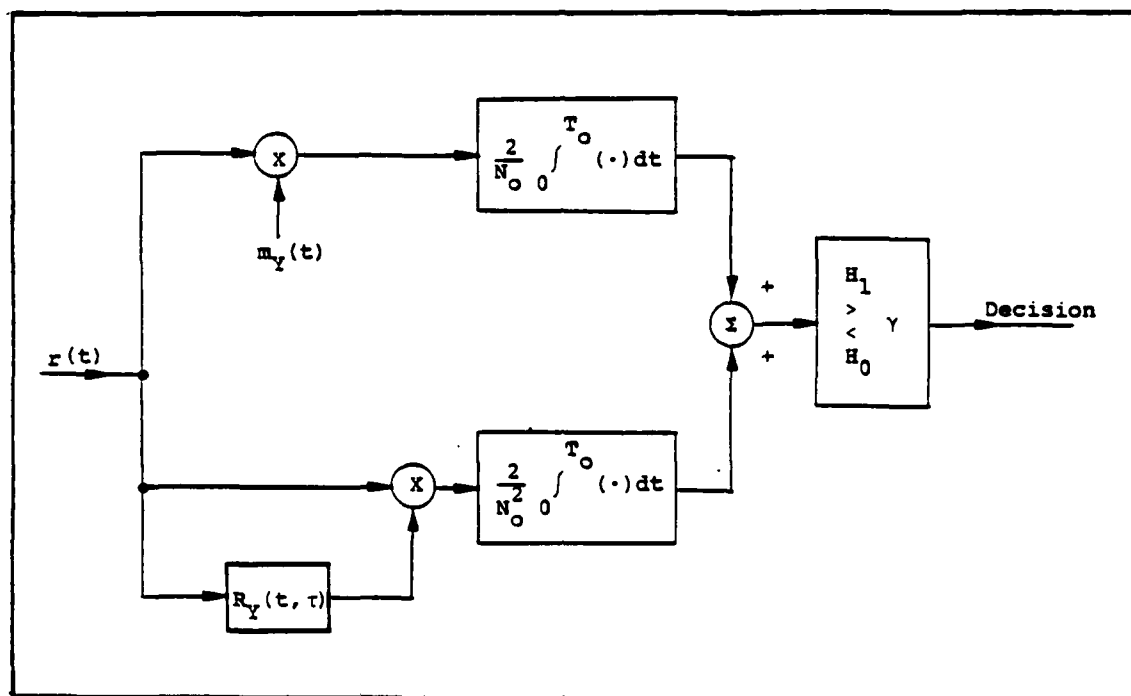


Fig. 2.6 Noncoherent Receiver (Nonuniform p.d.f., 3 Term Approximation)

$$\begin{aligned}
 m_Y(t) &= \frac{1}{T} \int_{-T/2}^{T/2} v(t-\lambda) d\lambda \\
 &= \frac{1}{T} \sum_{k=-\infty}^{\infty} v_k e^{j\frac{2\pi k}{T}t} \int_{-T/2}^{T/2} e^{-j\frac{2\pi k}{T}\lambda} d\lambda \\
 &= v_0
 \end{aligned} \tag{2.73}$$

which is a constant, and the autocorrelation function of $y(t)$ given by Equation (2.71) turns out to be

Note that $v(t)$ is a deterministic signal but as mentioned earlier, due to the r.v. λ ,

$$y(t) \stackrel{\Delta}{=} v(t-\lambda) \quad (2.69)$$

itself is a random process with expected value

$$E\{y(t)\} = \int_{-\infty}^{\infty} v(t-\lambda) f_{\Lambda}(\lambda) d\lambda \stackrel{\Delta}{=} m_Y(t) \quad (2.70)$$

and autocorrelation function

$$E\{y(t)y(\tau)\} = \int_{-\infty}^{\infty} v(t-\lambda)v(\tau-\lambda) f_{\Lambda}(\lambda) d\lambda \stackrel{\Delta}{=} R_Y(t, \tau) \quad (2.71)$$

Substitution of Equations (2.70) and (2.71) in Equation (2.68) leads to the following test that a receiver has to perform

$$\frac{2}{N_0} \int_0^{T_0} r(t) m_Y(t) dt + \frac{2}{N_0^2} \int_0^{T_0} r(t) \left[\int_0^{T_0} r(\tau) R_Y(t, \tau) d\tau \right] dt \underset{H_0}{\overset{H_1}{>}} \gamma \quad (2.72)$$

and the implementation of this receiver is shown in Fig. 2.6. Here the autocorrelation function $R_Y(t, \tau)$ can be considered as the impulse response of a filter that has to be designed for detection of the signal.

Furthermore, for the uniform p.d.f. on λ , the expected value of $y(t)$ given by Equation (2.70) becomes

$$\int_{-\infty}^{\infty} \exp\left\{\frac{2}{N_0} \int_0^{T_0} r(t)v(t-\lambda)dt\right\} \exp\left\{-\frac{1}{N_0} \int_0^{T_0} v^2(t-\lambda)dt\right\} f_{\Lambda}(\lambda) d\lambda \begin{matrix} H_1 \\ > \\ < \\ H_0 \end{matrix} \eta$$

where η is given by Equation (2.7). Note that the second exponential of the inequality given by Equation (2.11) has already been analyzed in Equations (2.14) through (2.16). Furthermore, if we expand the first exponential in the above inequality and approximate it with three terms as given by Equation (2.59), then the test of Equation (2.11) becomes

$$\begin{aligned} & \int_{-\infty}^{\infty} \frac{2}{N_0} \int_0^{T_0} r(t)v(t-\lambda)dt f_{\Lambda}(\lambda) d\lambda \\ & + \frac{1}{2} \int_{-\infty}^{\infty} \left[\frac{2}{N_0} \int_0^{T_0} r(t)v(t-\lambda)dt \right]^2 f_{\Lambda}(\lambda) d\lambda \begin{matrix} H_1 \\ > \\ < \\ H_0 \end{matrix} \gamma \end{aligned} \quad (2.67)$$

where γ is given by Equation (2.62).

Interchanging the order of integration in Equation (2.67), we obtain

$$\begin{aligned} & \frac{2}{N_0} \int_0^{T_0} r(t) \int_{-\infty}^{\infty} v(t-\lambda) f_{\Lambda}(\lambda) d\lambda dt \\ & + \frac{2}{N_0^2} \iint_0^{T_0} r(t)r(\tau) \int_{-\infty}^{\infty} v(t-\lambda)v(\tau-\lambda) f_{\Lambda}(\lambda) d\lambda dt d\tau \begin{matrix} H_1 \\ > \\ < \\ H_0 \end{matrix} \gamma \end{aligned} \quad (2.68)$$

$$E\{[r_n - E\{r_n|H_1, \lambda\}][r_m - E\{r_m|H_1, \lambda\}]|H_1, \lambda\} = \frac{N_0}{2} \Lambda_{nm} \quad (3.10)$$

so that

$$E\{\ell|H_1, \lambda\} = \sum_{n=1}^N \alpha_n(\lambda) \quad (3.11)$$

and

$$\begin{aligned} E\{[\ell - E\{\ell|H_1, \lambda\}]^2|H_1, \lambda\} \\ &= E\left\{\left[\sum_{n=1}^N \left(\int_0^{T_0} v(t-\lambda)v(t-\frac{nT}{N})dt + \int_0^{T_0} n(t)v(t-\frac{nT}{N})dt\right) - \sum_{n=1}^N \alpha_n(\lambda)\right]^2\right\} \\ &= E\left\{\left[\sum_{n=1}^N \int_0^{T_0} n(t)v(t-\frac{nT}{N})dt\right]^2\right\} \\ &= \frac{N_0}{2} \sum_{n=1}^N \sum_{m=1}^N \Lambda_{nm} = \sigma_\ell^2 \end{aligned} \quad (3.12)$$

Thus the conditional p.d.f.'s of ℓ are

$$f_L(\ell|H_0) = \frac{1}{\sqrt{2\pi\sigma_\ell^2}} e^{-\ell^2/2\sigma_\ell^2} \quad (3.13)$$

and

$$f_L(\ell | H_1, \lambda) = \frac{1}{\sqrt{2\pi\sigma_\ell^2}} e^{-\left(\ell - \sum_{n=1}^N \alpha_n(\lambda)\right)^2 / 2\sigma_\ell^2} \quad (3.14)$$

with

$$f_L(\ell | H_1) = \int_{-\infty}^{\infty} f_L(\ell | H_1, \lambda) f_\Lambda(\lambda) d\lambda \quad (3.15)$$

The detector of Fig. 3.1 performs the test

$$\begin{array}{c} H_1 \\ \ell > \gamma \\ < \\ H_0 \end{array} \quad (3.16)$$

so that its error probability, P_e is given by

$$P_e = P\{H_0\} \int_{\gamma}^{\infty} p_L(\ell | H_0) d\ell + P\{H_1\} \int_{-\infty}^{\gamma} p_L(\ell | H_1) d\ell \quad (3.17)$$

Let $p = P\{H_0\}$ and $1-p = P\{H_1\}$ so that using equations (3.13) and (3.15), equation (3.17) becomes

$$P_e = p \int_{\gamma}^{\infty} \frac{1}{\sqrt{2\pi\sigma_\ell^2}} e^{-\ell^2 / 2\sigma_\ell^2} d\ell + (1-p) \int_{-\infty}^{\gamma} \left[\int_{-\infty}^{\infty} \frac{1}{\sqrt{2\pi\sigma_\ell^2}} e^{-\left(\ell - \sum_{n=1}^N \alpha_n(\lambda)\right)^2 / 2\sigma_\ell^2} \cdot f_\Lambda(\lambda) d\lambda \right] d\ell \quad (3.18)$$

Interchanging the order of integration in the second (double) integral of equation (3.18), we obtain

$$\begin{aligned}
 & \int_{-\infty}^{\infty} f_{\Lambda}(\lambda) \left[\int_{-\infty}^{\gamma} \frac{1}{\sqrt{2\pi}\sigma_{\ell}} e^{-\frac{(\ell - \sum_{n=1}^N \alpha_n(\lambda))^2}{2\sigma_{\ell}^2}} d\ell \right] d\lambda \\
 &= \int_{-\infty}^{\infty} f_{\Lambda}(\lambda) \left[\int_{-\infty}^{\frac{\gamma - \sum_{n=1}^N \alpha_n(\lambda)}{\sigma_{\ell}}} \frac{1}{\sqrt{2\pi}} e^{-x^2/2} dx \right] d\lambda \\
 &= \int_{-\infty}^{\infty} f_{\Lambda}(\lambda) \operatorname{erf}\left(\frac{\gamma - \sum_{n=1}^N \alpha_n(\lambda)}{\sigma_{\ell}}\right) d\lambda \quad (3.19)
 \end{aligned}$$

Thus, the receiver probability of error becomes

$$P_e = p \operatorname{erfc}\left(\frac{\gamma}{\sigma_{\ell}}\right) + (1-p) \int_{-\infty}^{\infty} f_{\Lambda}(\lambda) \operatorname{erf}\left(\frac{\gamma - \sum_{n=1}^N \alpha_n(\lambda)}{\sigma_{\ell}}\right) d\lambda \quad (3.20)$$

The threshold γ can be optimized to minimize P_e . Such an approach unfortunately leads to a complicated integral equation that is not easily solvable. In practice however, P_e can be calculated on the computer for $\gamma = 0$, and then incrementing $|\gamma|$ until an optimum value of γ is found for a given SNR.

It must be pointed out that the receiver of Fig. 3.1 will not always yield desirable results. For example, if $v(t)$ is

sinusoidal, in the absence of noise, $\ell = 0$ which means that with noise present, the receiver is unable to detect the presence of the signal. Fortunately for $v(t)$ sinusoidal, a better receiver is available and its performance is well known [Ref. 4].

1. Special Case of Triangular Wave

Consider now a periodic waveform of triangular pulses and its two arbitrarily delayed versions as shown in Fig.

3.2. If we represent one triangular pulse by $p(t)$, then we can express $v(t)$ as

$$v(t) = \sum_{j=0}^M p(t-jT) \quad (3.21)$$

In order to find the cross correlation terms Λ_{nm} required for the computation of P_e [equation (3.19)], instead of taking all the pulses in equation (3.21), we simply consider the cross correlation of a single pulse of period T with a delayed version of itself and then multiply the result by the total number of pulses M within the interval T_0 , since $v(t)$ is assumed to be periodic with $MT = T_0$. In order to make computation simpler, Fig. 3.3 shows $p(t)$, $p(t-\alpha)$ and $p(t-\beta)$, where $\alpha < \beta$ has been assumed.

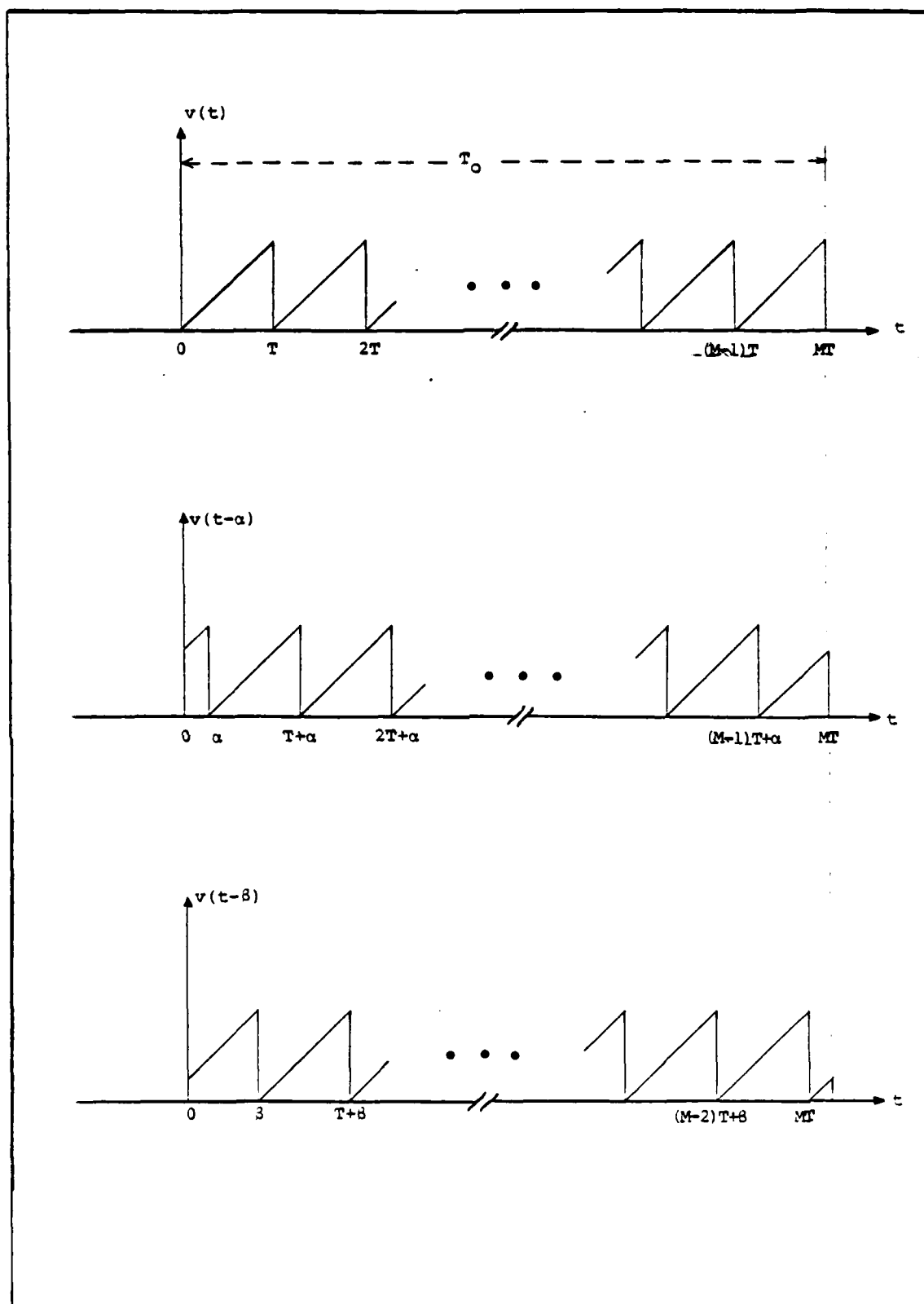


Fig. 3.2 Periodic Triangular Wave and Two of Its Delayed Versions

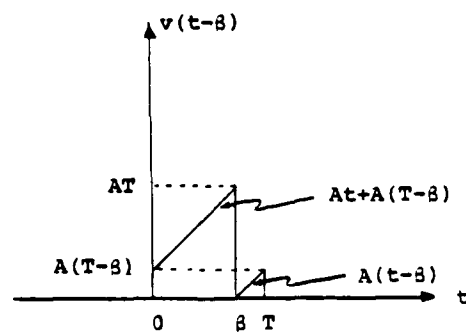
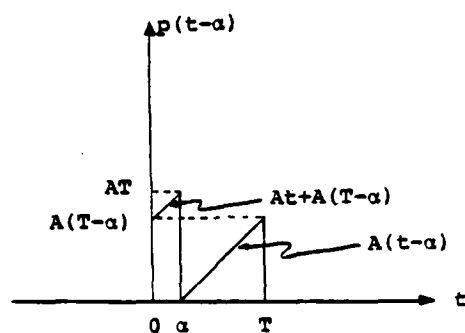
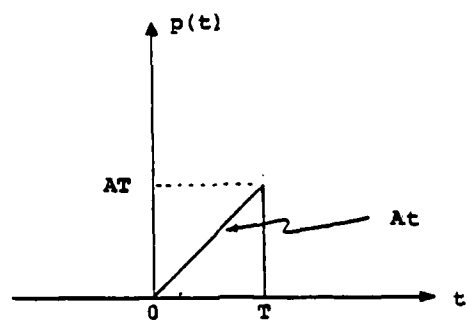


Fig. 3.3 One Period Restricted Triangular Wave and Two of Its Delayed Versions

Observe that for $\alpha < \beta$

$$\begin{aligned}
 \int_0^{T_0} v(t-\alpha)v(t-\beta)dt &= M \left[\int_0^\alpha p[t+(T-\alpha)]p[t+(T-\beta)]dt \right. \\
 &\quad \left. + \int_\alpha^\beta p(t-\alpha)p[t+(T-\beta)]dt + \int_\beta^T p(t-\alpha)p(t-\beta)dt \right] \\
 &= M \left[\int_0^\alpha [At+A(T-\alpha)][At+A(T-\beta)]dt \right. \\
 &\quad \left. + \int_\alpha^\beta A(t-\alpha)[At+A(T-\beta)]dt + \int_\beta^T A(t-\alpha)A(t-\beta)dt \right] \\
 &= MA^2 \left(\frac{\alpha^2 T}{2} + \frac{\alpha T^2}{2} - \alpha\beta T + \frac{\beta^2 T}{2} - \frac{\beta T^2}{2} + \frac{T^3}{3} \right) \\
 &\hspace{15em} (3.22)
 \end{aligned}$$

For $\alpha = \frac{nT}{N}$ and $\beta = \frac{mT}{N}$, equation (3.22) becomes

$$MA^2 T^3 \left(\frac{n^2}{2N^2} + \frac{n}{2N} - \frac{nm}{N^2} + \frac{m^2}{2N^2} - \frac{m}{2N} + \frac{1}{3} \right) = \Lambda_{nm} \quad (3.23)$$

provided $n < m$. For $n = m$ or equivalently $\alpha = \beta$, the quantity inside the parenthesis in equation (3.23) becomes $\frac{1}{3}$.

Similarly for $\alpha > \beta$, equation (3.22) becomes

$$\int_0^{T_0} v(t-\alpha)v(t-\beta)dt = MA^2 \left(\frac{\alpha^2 T}{2} - \frac{\alpha T^2}{2} - \alpha\beta T + \frac{\beta^2 T}{2} + \frac{\beta T^2}{2} + \frac{T^3}{3} \right) \quad (3.24)$$

Letting $\alpha = \frac{nT}{N}$ and $\beta = \frac{mT}{N}$ in equation (3.24), we obtain

$$\Lambda_{nm} = MA^2 T^3 \left(\frac{n^2}{2N^2} - \frac{n}{2N} - \frac{nm}{N^2} + \frac{m^2}{2N^2} + \frac{m}{2N} + \frac{1}{3} \right) \quad (3.25)$$

provided $n > m$. Here again for $n = m$, the quantity inside the parenthesis in equation (3.24) becomes $\frac{1}{3}$.

To proceed further with the analysis, the double summation of equation (3.8) is broken into three summations to account for $n < m$, $n = m$ and $n > m$. Thus

$$\sum_{n=1}^N \sum_{m=1}^N \Lambda_{nm} = \sum_{m=n+1}^N \sum_{n=1}^{N-1} \Lambda_{nm} + \sum_{n=1}^N \Lambda_{nn} + \sum_{n=m+1}^N \sum_{m=1}^{N-1} \Lambda_{nm} \quad (3.26)$$

Observe that the L.H.S. of equation (3.26) represents the sum of the elements of an $N \times N$ matrix. Whereas the middle term on the R.H.S. of this equation denotes the sum of the diagonal elements of the $N \times N$ matrix, the first term is the sum of all the elements in the upper triangular part and the third term is the sum of all the elements in the lower triangular part of the $N \times N$ matrix.

In order to evaluate the first term on the R.H.S. of equation (3.26), use of equation (3.23) ($n < m$ case) yields

$$\begin{aligned}
\sum_{n=1}^{N-1} \sum_{m=n+1}^N \Lambda_{nm} &= MA^2 T^3 \sum_{n=1}^{N-1} \sum_{m=n+1}^N \left\{ \frac{n^2}{2N^2} + \frac{n}{2N} - \frac{nm}{N^2} + \frac{m^2}{2N^2} - \frac{m}{2N} + \frac{1}{3} \right\} \\
&= MA^2 T^3 \left[\frac{1}{2N^2} \sum_{n=1}^{N-1} \sum_{m=n+1}^N n^2 + \frac{1}{2N} \sum_{n=1}^{N-1} \sum_{m=n+1}^N n \right. \\
&\quad - \frac{1}{N^2} \sum_{n=1}^{N-1} \sum_{m=n+1}^N nm + \frac{1}{2N^2} \sum_{n=1}^{N-1} \sum_{m=n+1}^N m^2 \\
&\quad \left. - \frac{1}{2N} \sum_{n=1}^{N-1} \sum_{m=n+1}^N m + \frac{1}{3} \sum_{n=1}^{N-1} \sum_{m=n+1}^N 1 \right] \\
&= MA^2 T^3 \left[\frac{3N^2 - 4N + 1}{24} \right] \tag{3.27}
\end{aligned}$$

The second term on the R.H.S. of equation (3.26) becomes

$$\sum_{n=1}^N \Lambda_{nn} = MA^2 T^3 \sum_{n=1}^N \frac{1}{3} = MA^2 T^3 \left[\frac{N}{3} \right] \tag{3.28}$$

since $\Lambda_{mn} = \frac{1}{3}$ for $n = m$.

Finally, substitution of equation (3.25) ($n > m$ case) in the third term on the R.H.S. of equation (3.26) yields

$$\begin{aligned}
\sum_{n=m+1}^N \sum_{m=1}^{N-1} \Lambda_{nm} &= MA^2 T^3 \left[\frac{n^2}{2N^2} - \frac{n}{2N} - \frac{nm}{N^2} + \frac{m^2}{2N^2} + \frac{m}{2N} + \frac{1}{3} \right] \\
&= MA^2 T^3 \left[\frac{3N^2 - 4N + 1}{24} \right] \tag{3.29}
\end{aligned}$$

Adding the results of equations (3.27), (3.28) and (3.29) yields

$$\sum_{n=1}^N \sum_{m=1}^N \Lambda_{nm} = MA^2 T^3 \left[\frac{3N^2 + 1}{12} \right] \quad (3.30)$$

Thus from equations (3.8) and (3.30), the conditional variance of ℓ becomes

$$\begin{aligned} \frac{N_0}{2} \sum_{n=1}^N \sum_{m=1}^N \Lambda_{nm} &= \frac{N_0}{2} MA^2 T^3 \left(\frac{3N^2 + 1}{12} \right) \\ &= \frac{N_0}{2} E \left(\frac{3N^2 + 1}{4} \right) \end{aligned} \quad (3.31)$$

since

$$\begin{aligned} \int_0^{T_0} v^2(t) dt &= M \int_0^T v^2(t) dt = M \int_0^T (At)^2 dt \\ &= \frac{MA^2 T^3}{3} \triangleq E \end{aligned} \quad (3.32)$$

is the energy of $v(t)$ for $0 \leq t \leq T_0$.

In order to compute the probability of error P_e , we need to evaluate $\sum_{n=1}^N \alpha_n(\lambda)$ given by equations (3.9) and (3.11) as

$$\sum_{n=1}^N \alpha_n(\lambda) = \sum_{n=1}^N \int_0^{T_0} v(t-\lambda) v(t - \frac{nT}{N}) dt \quad (3.33)$$

A Fourier series expansion of $v(t-\lambda)$ and $v(t - \frac{nT}{N})$ yields

$$\begin{aligned} \sum_{n=1}^N \alpha_n(\lambda) &= \sum_{n=1}^N \sum_{k=-\infty}^{\infty} \sum_{\ell=-\infty}^{\infty} v_k v_{\ell} e^{-j\frac{2\pi}{T}k\lambda} e^{-j2\pi\frac{\ell n}{N}} \int_0^{T_0} e^{j\frac{2\pi}{T}(k+\ell)t} dt \\ &= T_0 \sum_{k=-\infty}^{\infty} |v_k|^2 e^{-j\frac{2\pi}{T}k\lambda} \sum_{n=1}^N e^{jn(\frac{2\pi k}{N})} \end{aligned} \quad (3.34)$$

Observe that for $k = \pm iN$, where i is an integer, the second summation involving the index n yields N , otherwise it yields zero.

Thus, equation (3.33) can be written as

$$\begin{aligned} \sum_{n=1}^N \alpha_n(\lambda) &= T_0 N \left(|v_0|^2 + \sum_{k=-\infty}^{-1} |v_{kN}|^2 e^{-j\frac{2\pi}{T}kN\lambda} \right. \\ &\quad \left. + \sum_{k=1}^{\infty} |v_{kN}|^2 e^{-j\frac{2\pi}{T}kN\lambda} \right) \\ &= T_0 N (|v_0|^2 + 2 \sum_{k=1}^{\infty} |v_{kN}|^2 \cos \frac{2\pi}{T}kN\lambda) \end{aligned} \quad (3.35)$$

since

$$|v_k|^2 = |v_{-k}|^2$$

In equation (3.6), if we represent $v(t - \frac{nT}{N})$ and $v(t - \frac{mT}{N})$ in terms of Fourier series, then

$$\begin{aligned}
 \sum_{n=1}^N \sum_{m=1}^N \Lambda_{nm} &= \sum_{n=1}^N \sum_{m=1}^N \sum_{k=-\infty}^{\infty} \sum_{\ell=-\infty}^{\infty} v_k v_{\ell} e^{-j\frac{2\pi kn}{N}} e^{-j\frac{2\pi \ell m}{N}} \int_0^{T_0} e^{j\frac{2\pi}{T}(k+\ell)t} dt \\
 &= T_0 \sum_{k=-\infty}^{\infty} |v_k|^2 \sum_{n=1}^N e^{jn(-\frac{2\pi k}{N})} \sum_{m=1}^N e^{jm(\frac{2\pi k}{N})} \\
 &= T_0 \sum_{k=-\infty}^{\infty} |v_k|^2 \left[\frac{\sin(k\pi)}{\sin(\frac{k\pi}{N})} \right]^2 \quad (3.36)
 \end{aligned}$$

since

$$\sum_{n=1}^N e^{jn\theta} = \frac{\sin(N\theta/2)}{\sin(\theta/2)} e^{j(N+1)\theta/2} \quad (3.37)$$

Observe that the R.H.S. of equation (3.36) is always zero except for $k = \pm iN$ where i is an integer. Also observe that for $k = \pm iN$, the R.H.S. of equation (3.36) becomes an indeterminate form. Due to that reason, differentiating $\sin(k\pi)$ and $\sin(\frac{k\pi}{N})$ w.r.t. k and then taking the limit $k \rightarrow iN$, equation (3.36) becomes

$$\begin{aligned}
 \sum_{n=1}^N \sum_{m=1}^N \Lambda_{nm} &= T_0 N^2 \sum_{k=-\infty}^{\infty} |v_{kN}|^2 \\
 &= T_0 N^2 (v_0^2 + 2 \sum_{k=1}^{\infty} |v_{kN}|^2) \quad (3.38)
 \end{aligned}$$

so that equation (3.8) can be written as

$$\sigma_{\ell}^2 = \frac{N_0}{2} T_0 N^2 (V_0^2 + 2 \sum_{k=1}^{\infty} |V_{kN}|^2) \quad (3.39)$$

Equations (3.35) and (3.39) are of general form and can be applied to any signal, not just a triangular waveform.

The Fourier coefficients V_k of the periodic triangular wave are

$$V_k = \begin{cases} \frac{AT}{2} & k = 0 \\ \frac{jAT}{2\pi k} & \text{otherwise} \end{cases} \quad (3.40)$$

and

$$|V_k|^2 = \begin{cases} \frac{A^2 T^2}{4} & k = 0 \\ \frac{A^2 T^2}{4\pi^2 k^2} & \text{otherwise} \end{cases} \quad (3.41)$$

so that the use of equations (3.31) and (3.35) yields

$$\frac{\gamma}{\sigma_{\ell}} = \frac{\gamma}{[N_0 E(\frac{3N^2+1}{8})]^{1/2}} = \frac{\gamma^*}{[\frac{E}{N_0}(\frac{3N^2+1}{8})]^{1/2}} \quad (3.42)$$

where $\gamma^* = \gamma/N_0$

$$\begin{aligned}
\frac{\sum_{n=1}^N \alpha_n(\lambda)}{\sigma_\ell} &= \sqrt{\frac{E}{N_O} \left(\frac{8}{3N^2 + 1} \right)} \left[\frac{N \left(\frac{A^2 T^2}{4} + 2 \sum_{k=1}^{\infty} \frac{A^2 T^2 \cos k \frac{2\pi}{T} N \lambda}{4\pi^2 N^2 k^2} \right)}{\frac{A^2 T^2}{4} + 2 \sum_{k=1}^{\infty} \frac{A^2 T^2}{4\pi^2 k^2 N^2}} \right] \\
&= \sqrt{\frac{E}{N_O} \left(\frac{8}{3N^2 + 1} \right)} \left[\frac{N \left\{ 1 + \frac{2}{N^2} \left[\frac{1}{6} - \frac{\lambda}{T} + \left(\frac{\lambda}{T} \right)^2 \right] \right\}}{1 + 1/3N^2} \right] \quad (3.43)
\end{aligned}$$

since

$$\sum_{k=1}^{\infty} \frac{\cos k\theta}{k^2} = \frac{\pi^2}{6} - \frac{\pi}{2} \theta + \frac{\theta^2}{4} \quad 0 \leq \theta \leq 2\pi \quad (3.44)$$

and

$$\begin{aligned}
\frac{\gamma - \sum_{n=1}^N \alpha_n(\lambda)}{\sigma_\ell} &= \frac{\gamma^*}{\left[\frac{E}{N_O} \left(\frac{3N^2 + 1}{8} \right) \right]^{1/2}} - \sqrt{\frac{E}{N_O} \left(\frac{8}{3N^2 + 1} \right)} \\
&\quad \times \left[\frac{N \left\{ 1 + \frac{2}{N^2} \left[\frac{1}{6} - \frac{\lambda}{T} + \left(\frac{\lambda}{T} \right)^2 \right] \right\}}{1 + 1/3N^2} \right] \quad (3.45)
\end{aligned}$$

Finally, the expression for P_e , after substituting equations (2.1), (3.42) and (3.44) in equation (3.20), becomes

Figure 4.1 shows the performance of this receiver as a function of SNR. This graph was obtained through numerical evaluation of Equation (2.40) under the assumption that $v(t)$ has a strong DC component in comparison to its harmonics, equal prior probabilities, and uniform p.d.f. on the r.v. λ . Due to the constraint imposed by Equation (2.20), Equation (2.40) is valid up to an SNR of about -4.1 dB. Thus Fig. 4.1 is plotted only up to the SNR of -4.1 dB.

Observe that P_e is at a very high level of about 0.3. However, it decreases as SNR increases, as expected. While it is clear that no receiver could operate with an error probability of 0.3, the figure does give an indication of the performance level that can be expected at low SNR's. For high SNR's, it is expected that P_e will continue to decrease to reasonable levels. However, for high SNR's, the receiver of Fig. 2.2 is no longer optimum.

2. Receiver Operating on Arbitrary Signals (Nonuniform p.d.f. on λ)

The two-term approximation on the exponential appearing in Equation (2.19) and application of the nonuniform p.d.f. on λ given by Equation (2.1) resulted in the receiver of Fig. 2.4 that could operate on signals having either zero or non-zero DC component. Observe that as $m \rightarrow 0$, the receiver of Fig. 2.4 becomes equal to the receiver of Fig. 2.2. Two specific signals, a sine wave and square wave, both having zero DC component, were analyzed.

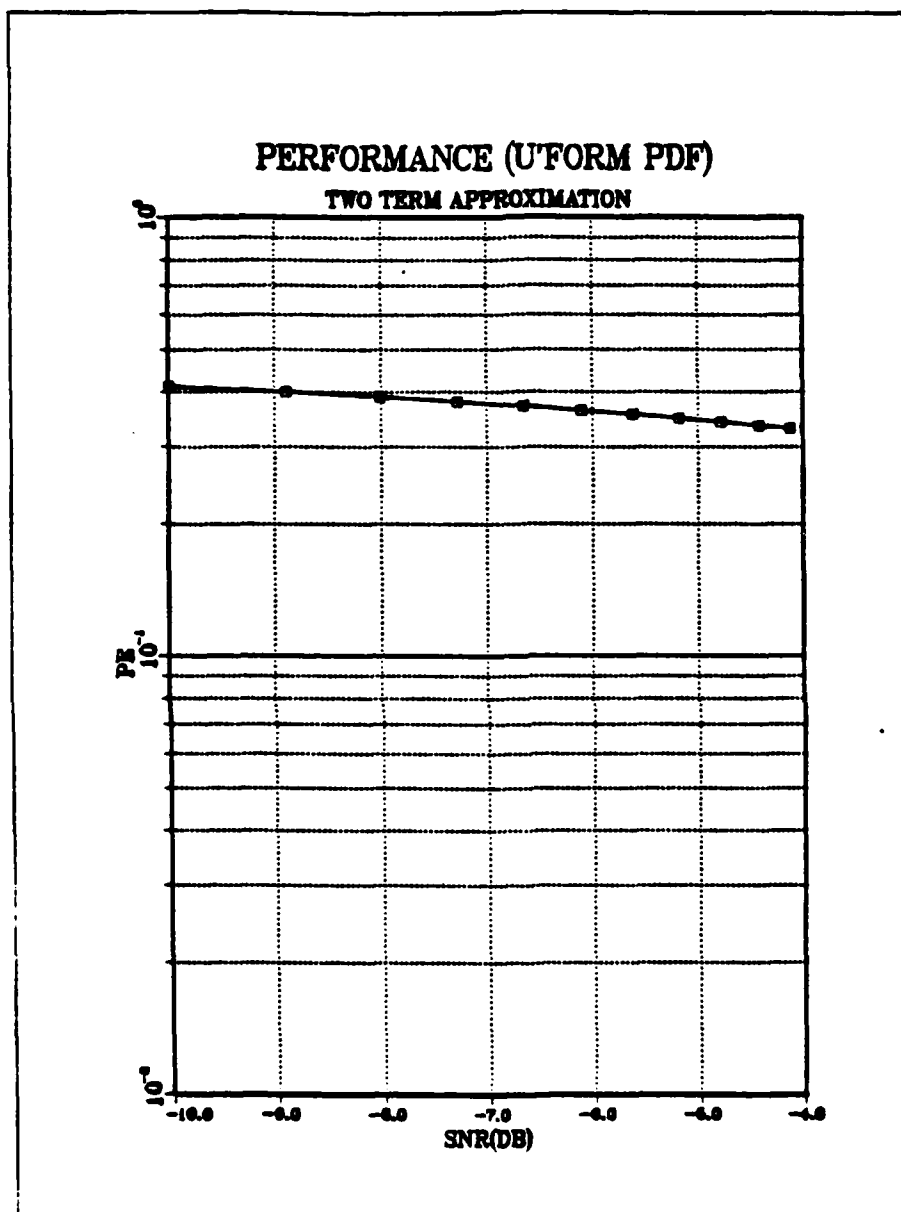


Figure 4.1 Performance (Uniform p.d.f.)

IV. DISCUSSION OF GRAPHICAL RESULTS

This chapter presents graphical results obtained by applying the analytical results of the previous chapters to specific examples and carrying out the required computations on the computer. The plots are intended to display receiver performance in terms of probability of error (P_e) as a function of SNR. Some curves of P_e versus comparator threshold level have also been included in order to show the dependency of P_e on the threshold which in turn depends on SNR. The graphical results displaying performance of the optimum receivers are presented first, followed by graphical results displaying performance of the suboptimum receivers analyzed.

A. GRAPHICAL RESULTS FOR OPTIMUM RECEIVERS

1. Receivers Operating on Signals with Nonzero DC Component (Uniform p.d.f. on λ)

In Chapter II, using statistical communication theoretic principles, a simple integrator receiver (Fig. 2.2) was derived that could discriminate between signal plus noise and noise only hypotheses provided the signal had a non-zero DC component. Recall that the receiver derivation and the subsequent performance evaluation carried out was made possible by the two-term approximation on the exponential appearing in Equation (2.19). Equivalently, low SNR conditions were assumed so that the P_e results are only valid for low SNR's.

summation in equations (3.35) and (3.61) turned out to be of such a form that it could be expressed in closed form. . For the sine wave, summation disappeared due to the fact that its coefficients V_k exist only for $k = \pm 1$. These results in the form of graphs are presented and discussed in Chapter IV.

so that equation (3.59) becomes

$$\begin{aligned}
 \frac{m(\lambda)}{\sigma_\ell} &= \sqrt{2E/N_0} \frac{\sum_{k=1}^{\infty} \frac{\cos k2\pi(\frac{\lambda-\alpha}{T})}{k^2}}{\sum_{\ell=1}^{\infty} \frac{1}{\ell^2}} \\
 &= \sqrt{2E/N_0} \frac{\pi^2 (\frac{1}{6} - (\frac{\lambda-\alpha}{T}) + (\frac{\lambda-\alpha}{T})^2)}{\pi^2/6} \\
 &= \sqrt{2E/N_0} (1 - 6(\frac{\lambda-\alpha}{T}) + 6(\frac{\lambda-\alpha}{T})^2) \quad (3.69)
 \end{aligned}$$

Therefore

$$\begin{aligned}
 P_e &= \frac{1}{2} \left\{ \text{erfc}\left(\frac{\gamma^*}{\sqrt{E/2N_0}}\right) + \frac{1}{T_0(m)T} \int_{-T/2}^{T/2} e^{m \cos \frac{2\pi\lambda}{T}} \right. \\
 &\quad \left. \text{erf}\left(\frac{\gamma^*}{\sqrt{E/2N_0}} - \sqrt{2E/N_0} (1 - 6(\frac{\lambda-\alpha}{T}) + 6(\frac{\lambda-\alpha}{T})^2) d\ell \right) d\ell \right\} \quad (3.70)
 \end{aligned}$$

Observe that equations (3.35) and (3.62) involve summations whose indices run from 1 to infinity. In practice, it is not possible to compute infinite sums. However, due to the fact that for all reasonable signals $v(t)$, the magnitude of the V_k coefficients gets smaller as k gets bigger, this infinite sum can be truncated without introducing significant computational error.

Fortunately for triangular and square wave signals considered as special cases in this chapter, the argument of

Thus equation (3.60) becomes

$$\frac{m(\lambda)}{\sigma_{\lambda}} = \sqrt{2E/N_0} \frac{\frac{A^2}{2} \cos \frac{2\pi}{T}(\lambda-\alpha)}{A^2/2} = \sqrt{2E/N_0} \cos \frac{2\pi}{T}(\lambda-\alpha) \quad (3.6.6)$$

and for $p = (1-p) = \frac{1}{2}$, equation (3.58) becomes

$$P_e = \frac{1}{2} \left\{ \operatorname{erfc}^*\left(\frac{\gamma^*}{\sqrt{E/2N_0}}\right) + \frac{1}{T I_0(m)} \int_{-T/2}^{T/2} e^{m \cos \frac{2\pi \lambda}{T}} \times \operatorname{erf}^*\left(\frac{\gamma^*}{\sqrt{E/2N_0}} - \sqrt{2E/N_0} \cos \frac{2\pi}{T}(\lambda-\alpha)\right) d\lambda \right\} \quad (3.67)$$

As mentioned earlier in Chapter II, $m = 0$ corresponds to a uniform p.d.f. on λ , i.e. $p(\lambda) = \frac{1}{T}$, so that the error probability expression for $m = 0$ becomes

$$P_e = \frac{1}{2} \left\{ \operatorname{erfc}^*\left(\frac{\gamma^*}{\sqrt{E/2N_0}}\right) + \frac{1}{T} \int_{-T/2}^{T/2} \operatorname{erf}^*\left(\frac{\gamma^*}{\sqrt{E/2N_0}} - \sqrt{2E/N_0} \cos \frac{2\pi}{T}(\lambda-\alpha)\right) d\lambda \right\} \quad (3.68)$$

2. Square Wave

Consider now the second special case in which $v(t)$ is a periodic square wave as shown in Fig. 2.6. In Chapter II we showed that

$$|v_k|^2 = \begin{cases} \left(\frac{2A}{k\pi}\right)^2 & \text{for } k = \text{odd} \\ 0 & \text{for } k = \text{even} \end{cases}$$

As before, determination of the optimum threshold by solution of $\frac{dp}{d\gamma} = 0$ involves solving an equation of a form similar to that of equation (3.47).

In general, solutions in closed form do not appear tractable. A search for an optimum γ may be performed or solutions for specific cases may be possible. This is illustrated by considering two special cases in which $v(t)$ is a

1. sine wave
2. square wave.

1. Sine Wave

As a first special case, let

$$\begin{aligned} v(t) &= A \cos \frac{2\pi}{T}t \\ &= \frac{A}{2} e^{j\frac{2\pi}{T}t} + \frac{A}{2} e^{-j\frac{2\pi}{T}t} \end{aligned} \quad (3.63)$$

so that

$$v_k = \begin{cases} \frac{A}{2} & |k| = 1 \\ 0 & \text{otherwise} \end{cases} \quad (3.64)$$

and

$$2 \sum_{k=1}^{\infty} |v_k|^2 = 2 \frac{A^2}{4} = \frac{A^2}{2} \quad (3.65)$$

Since the receiver was not designed from likelihood ratio test principles, the threshold γ must be set for minimum P_e .

The approach used to find the optimum threshold involves

solving $\frac{dP_e}{d\gamma} = 0$ for γ as before.

Since

$$\frac{\gamma}{\sigma_\ell} = \frac{\gamma}{\sqrt{N_0 E/2}} = \frac{\gamma^*}{\sqrt{E/2N_0}} \quad \text{where } \gamma^* = \gamma/N_0 \quad (3.59)$$

and

$$\frac{m(\lambda)}{\sigma_\ell} = \sqrt{2E/N_0} \left\{ \frac{|v_0|^2 + 2 \sum_{k=1}^{\infty} |v_k|^2 \cos \frac{2\pi k}{T}(\alpha - \lambda)}{|v_0|^2 + 2 \sum_{\ell=1}^{\infty} |v_\ell|^2} \right\} \quad (3.60)$$

we have

$$\frac{\gamma - m(\lambda)}{\sigma_\ell} = \frac{\gamma^*}{\sqrt{E/2N_0}} - \sqrt{2E/N_0} \left\{ \frac{|v_0|^2 + 2 \sum_{k=1}^{\infty} |v_k|^2 \cos \frac{2\pi k}{T}(\lambda - \alpha)}{|v_0|^2 + 2 \sum_{\ell=1}^{\infty} |v_\ell|^2} \right\} \quad (3.61)$$

Thus equation (3.56) becomes

$$P_e = p \operatorname{erfc}^*\left(\frac{\gamma}{\sqrt{E/2N_0}}\right) + (1-p) \int_{-T/2}^{T/2} \frac{e^{m \cos \frac{2\pi \lambda}{T}}}{T I_0(m)} \times \operatorname{erf}^* \left(\frac{\gamma^*}{\sqrt{E/2N_0}} - \sqrt{2E/N_0} \left\{ \frac{|v_0|^2 + 2 \sum_{k=1}^{\infty} |v_k|^2 \cos \frac{2\pi k}{T}(\lambda - \alpha)}{|v_0|^2 + 2 \sum_{\ell=1}^{\infty} |v_\ell|^2} \right\} \right) d\lambda \quad (3.62)$$

so that

$$f_L(\ell|H_1) = \int_{-\infty}^{\infty} \frac{1}{\sqrt{2\pi}\sigma_\ell} e^{-[\ell-m(\lambda)]^2/2\sigma_\ell^2} f_\Lambda(\lambda) d\lambda \quad (3.56)$$

Thus the expression for P_e is given by

$$\begin{aligned} P_e &= P\{\ell > \gamma|H_0\}P\{H_0\} + P\{\ell < \gamma|H_1\}P\{H_1\} \\ &= p \int_{\gamma}^{\infty} \frac{1}{\sqrt{2\pi}\sigma_\ell} e^{-\ell^2/2\sigma_\ell^2} d\ell + (1-p) \int_{-\infty}^{\gamma} \int_{-\infty}^{\infty} \frac{1}{\sqrt{2\pi}\sigma_\ell} e^{-(\ell-m(\lambda))^2/2\sigma_\ell^2} \\ &\quad \times f_\Lambda(\lambda) d\lambda d\ell \end{aligned} \quad (3.57)$$

where

$$p = P\{H_0\} \quad \text{and} \quad (1-p) = P\{H_1\}$$

as before.

After a change of variables, equation (3.57) can be written as

$$\begin{aligned} P_e &= p \int_{\gamma/\sigma_\ell}^{\infty} \frac{1}{\sqrt{2\pi}} e^{-x^2/2} + (1-p) \int_{-\infty}^{\infty} \int_{-\infty}^{\infty} \frac{1}{\sqrt{2\pi}} e^{-x^2/2} dx f_\Lambda(\lambda) d\lambda \\ &= p \operatorname{erfc}\left(\frac{\gamma}{\sigma_\ell}\right) + (1-p) \int_{-\infty}^{\infty} f_\Lambda(\lambda) \operatorname{erf}\left(\frac{\gamma-m(\lambda)}{\sigma_\ell}\right) d\lambda \end{aligned} \quad (3.58)$$

Also

$$\begin{aligned}
 E\{\ell | H_1, \lambda\} &= \int_0^{T_0} v(t-\lambda) v(t-\alpha) dt \\
 &= \sum_{k=-\infty}^{\infty} \sum_{\ell=-\infty}^{\infty} v_k v_{\ell} e^{-j\frac{2\pi}{T}(k\lambda+\ell\alpha)} \int_0^{T_0} e^{j\frac{2\pi}{T}(k+\ell)t} dt \\
 &= T_0 \sum_{k=-\infty}^{\infty} |v_k|^2 e^{-j\frac{2\pi}{T}k(\lambda-\alpha)} \\
 &= T_0 [|v_0|^2 + 2 \sum_{k=1}^{\infty} |v_k|^2 \cos \frac{2\pi}{T}k(\lambda-\alpha)] \triangleq m(\lambda)
 \end{aligned} \tag{3.52}$$

It can be shown without a great deal of difficulty that

$$\text{Var}\{\ell | H_1, \lambda\} = \sigma_{\ell}^2 \tag{3.53}$$

Therefore the conditional p.d.f.'s of ℓ are given by

$$f_L(\ell | H_0) = \frac{1}{\sqrt{2\pi}\sigma_{\ell}} e^{-\ell^2/2\sigma_{\ell}^2} \tag{3.54}$$

$$f_L(\ell | H_1, \lambda) = \frac{1}{\sqrt{2\pi}\sigma_{\ell}} e^{-[\ell - m(\lambda)]^2/2\sigma_{\ell}^2} \tag{3.55}$$

Thus

$$\ell = \int_0^{T_0} r(t)v(t-\alpha)dt \quad (3.49)$$

where $\alpha = \frac{T}{N}, \frac{2T}{N}, \frac{3T}{N}, \dots, T$ and α may take on only one such value for $0 \leq t \leq T_0$. In order to determine receiver performance, we note that ℓ is a conditionally Gaussian random variable with

$$E\{\ell|H_0\} = 0 \quad (3.50)$$

$$\begin{aligned} \text{Var}\{\ell|H_0\} &= E\left\{\left[\int_0^{T_0} n(t)v(t-\alpha)dt\right]^2\right\} \\ &= \frac{N_0}{2} \int_0^{T_0} v^2(t-\alpha)dt \\ &= \frac{N_0}{2} \sum_{k=-\infty}^{\infty} \sum_{\ell=-\infty}^{\infty} v_k v_{\ell} e^{-j\frac{2\pi}{T}(k+\ell)\alpha} \int_0^{T_0} e^{j\frac{2\pi}{T}(k+\ell)t} dt \\ &= \frac{N_0 T_0}{2} \sum_{k=-\infty}^{\infty} |v_k|^2 = \frac{N_0}{2} E \triangleq \sigma_{\ell}^2 \end{aligned} \quad (3.51)$$

where v_k are the exponential Fourier series coefficients of $v(t)$, and E is the energy of $v(t)$ for $0 \leq t \leq T$.

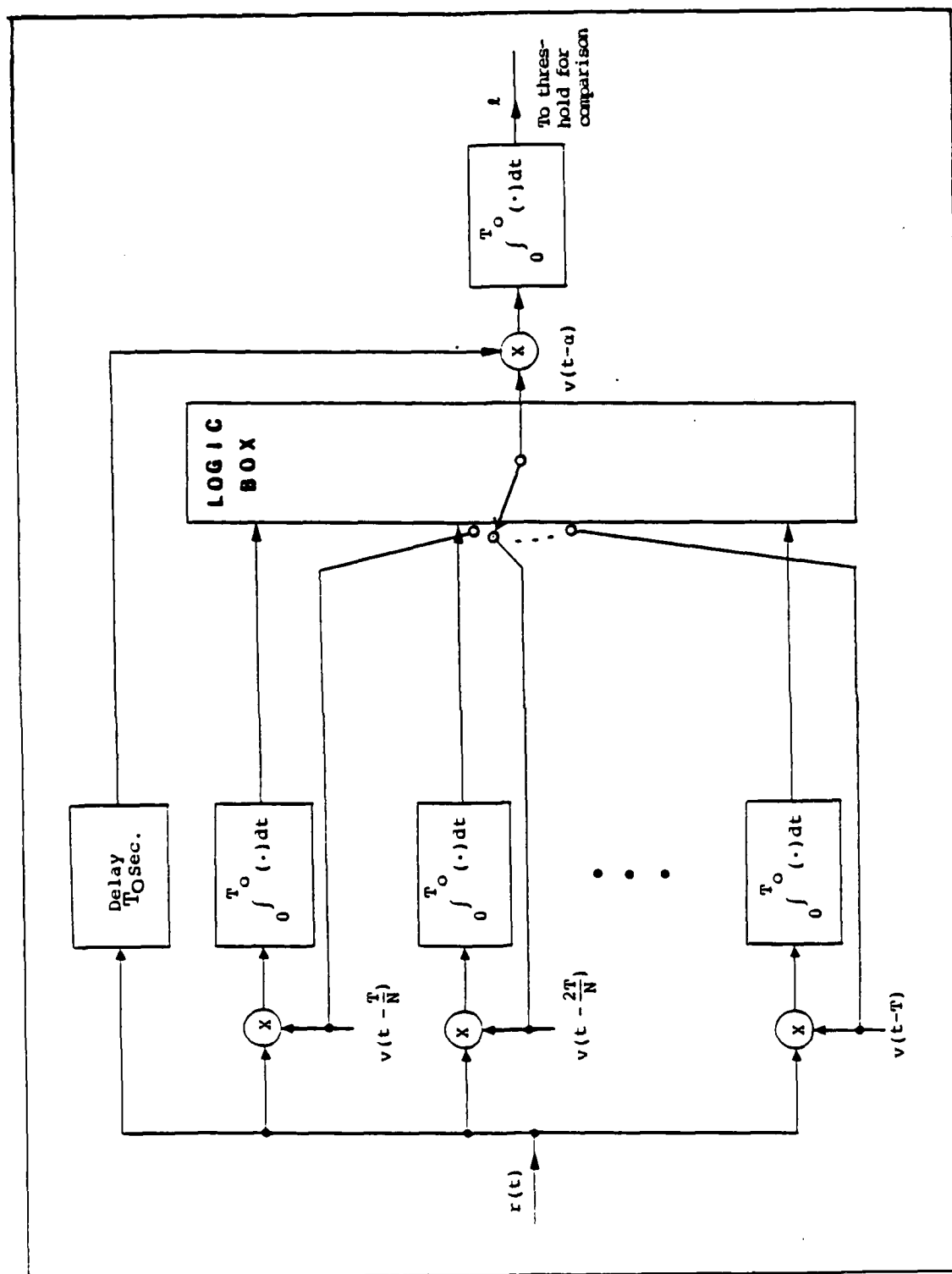


Fig. 3.4 Noncoherent Correlator Receiver

Clearly, the computer could be used to search for a value of γ that satisfies the equality prescribed in equation (3.48).

The approach that has been used in trying to obtain the optimum threshold involves using the computer to evaluate equation (3.46) as a function of γ for fixed SNR. Thus the value of γ for which P_e is minimum yields the optimum threshold for that particular value of SNR. This procedure is repeated for different values of SNR. The resulting values are then used to plot P_e vs. SNR. These curves have been plotted using optimum threshold settings and the results have been summarized and discussed in Chapter IV. (Observe that the threshold γ is SNR dependent. This situation is typical of noncoherent signal detection problems.)

B. ESTIMATOR-CORRELATOR RECEIVER

The second suboptimum receiver being proposed is the receiver structure shown in Fig. 3.4. It is basically an estimator-correlator receiver in which first a coarse estimate of the time delay in $v(t)$ is made and then this information is used to process the delayed signal $r(t)$ coherently with an estimated reference.

In this receiver the largest output of the N correlator branches is used as an estimate of the signal phase by the logic choice. This estimate is used to provide an accurate local reference with which to perform the correlation detection operation. The output ℓ of the main correlator is used for threshold comparison in order to make the decisions.

$$P_e = p \operatorname{erfc}^* \left(\frac{\gamma^*}{\left[\frac{E}{N_0} \frac{(3N^2+1)}{8} \right]^{1/2}} \right) + (1-p) \int_{-T/2}^{T/2} \frac{e^{\frac{m \cos \frac{2\pi \lambda}{T}}{T I_0(m)}}}{\sqrt{2\pi\sigma_\ell^2}} d\lambda$$

$$\operatorname{erf}^* \left(\frac{\gamma^*}{\left[\frac{E}{N_0} \frac{(3N^2+1)}{8} \right]^{1/2}} - \sqrt{\frac{E}{N_0} \frac{8}{3N^2+1}} \right)$$

$$\left[\frac{3N^3 + 6N \left[\frac{1}{6} - \frac{\lambda}{T} + \left(\frac{\lambda}{T} \right)^2 \right]}{(3N^2+1)} \right] d\lambda \quad (3.46)$$

As mentioned earlier, the receiver of Fig. 3.1 has been designed via ad-hoc methods, so that the optimum threshold setting is not readily obtainable. The difficulty in applying an analytical approach to the problem of finding the optimum threshold arises in the solution of $\frac{dP_e}{d\gamma} = 0$ for γ . Since

$$\frac{dP_e}{d\gamma} = -p \frac{1}{\sqrt{2\pi\sigma_\ell^2}} e^{-\frac{\gamma^2}{2\sigma_\ell^2}} + (1-p) \int_{-T/2}^{T/2} f_\Lambda(\lambda) \frac{1}{\sqrt{2\pi\sigma_\ell^2}} e^{-\frac{(\gamma - \sum_{n=1}^N \alpha_n(\lambda))^2}{2\sigma_\ell^2}} d\lambda \quad (3.47)$$

then, solution of $\frac{dP_e}{d\gamma} = 0$ is equivalent to solving

$$\int_{-T/2}^{T/2} f_\Lambda(\lambda) e^{-\frac{\gamma \sum_{n=1}^N \alpha_n(\lambda)}{\sigma_\ell^2}} e^{-\frac{[\sum_{n=1}^N \alpha_n(\lambda)]^2}{2\sigma_\ell^2}} d\lambda = \frac{p}{(1-p)} \quad (3.48)$$

Figure 4.2, obtained through numerical evaluation of Equation (2.80), shows the performance of this receiver as a function of SNR when $v(t)$ is a sine wave. Three different values of the independent parameter m were considered. Recall that m controls the level of uncertainty about the time delay λ . As expected, as m increases, P_e decreases for a given SNR. For example, an SNR of -5.2 dB is required in order to achieve a P_e of 0.4 at $m = 2$. With $m = 90$, we need an SNR of -9 dB to achieve the same P_e . Note that the $m = 0$ case has not been considered here due to the fact that $m = 0$ corresponds to a uniform p.d.f. on λ . The receiver for that case (Fig. 2.4) is unable to detect signals having zero DC component, resulting in P_e equal to 0.5.

Curves shown in Fig. 4.3 are the result of numerical evaluation of Equation (2.90) in which three different values of the independent parameter m have been considered. The $m = 0$ case has not been considered here either due to the same reasons presented for the sine wave case.

Observe that Equation (2.90) involves the computation of infinite sums which can not be carried out in practice. However, due to the fact that for all finite power signals $v(t)$, the magnitude of the V_k coefficients gets smaller as k gets bigger and thus, truncation is possible. Inclusion of more coefficients in Equation (2.90) corresponds to increased accuracy in the results. Furthermore, P_e changes as k is incremented, however up to a point only as further increase in

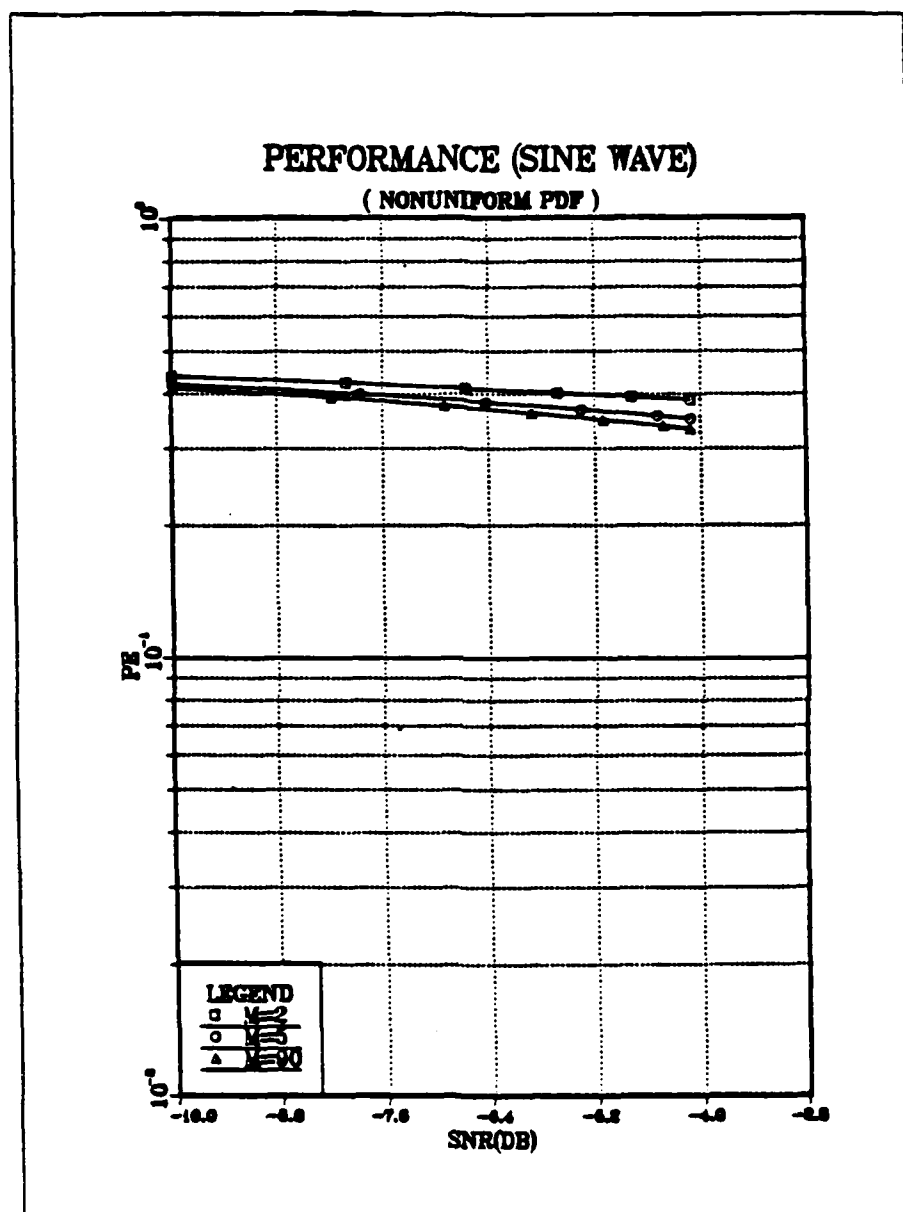


Figure 4.2 Performance (Sine Wave)

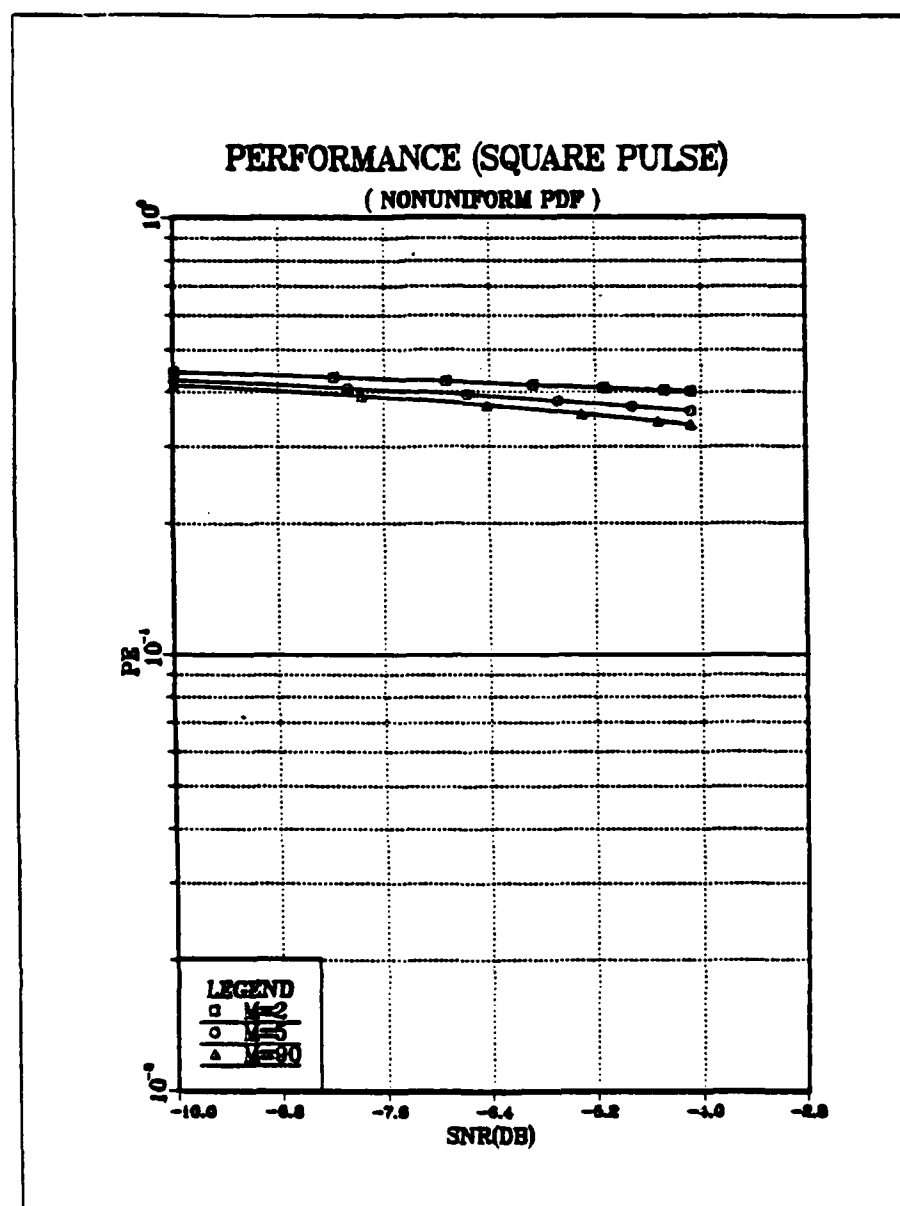


Figure 4.3 Performance (Square Wave)

k beyond this limit do not result in an appreciable change in P_e . This phenomenon is illustrated in Table I.

TABLE I	
PROBABILITY OF ERROR VS # OF COEFFICIENTS SUMMED (SNR = -10 DB)	
# OF COEFFICIENTS SUMMED	PROBABILITY OF ERROR
1	0.445124370+00
2	0.444339470+00
3	0.444325590+00
4	0.444325430+00
5	0.444325420+00
6	0.444325420+00
7	0.444325420+00
8	0.444325420+00
9	0.444325420+00
10	0.444325420+00

We see that P_e keeps on decreasing until the number of coefficients summed is 5. For $k > 5$, P_e remains unchanged. Thus, for this example the computation of Equation (2.90) was carried out with sums truncated to 5 terms. The performance curves for the square wave signal are shown in Fig. 4.3 for low SNR conditions. With $m = 2$, an SNR of -4.1 dB is required in order to achieve a P_e of 0.4 while for the same P_e , with $m = 90$, the SNR required is -8.8 dB.

B. GRAPHICAL RESULTS FOR SUBOPTIMUM RECEIVERS

In Chapter III, two suboptimum receivers were analyzed. The design approach used in that chapter was different in the sense that receivers were derived via strictly heuristic

means. Therefore, the optimum threshold setting for the receiver was not readily obtainable. However, a computational approach was used to solve the problem of properly setting the threshold prior to evaluating P_e as a function of SNR.

1. N-Correlator Receiver

The first suboptimum receiver analyzed in Chapter III was the N-Correlator receiver of Fig. 3.1, and its performance with $v(t)$ a periodic triangular pulse was evaluated. The graphical results corresponding to the numerical evaluation of Equation (3.46) are shown in Figs. 4.4 through 4.12. As mentioned earlier, using the computer, Equation (3.46) has been evaluated as a function of the threshold γ for fixed SNR values starting at -10 dB and increasing in increments of 5 dB. For a given SNR, the threshold value for which P_e is minimum corresponds to the optimum threshold for that particular SNR. These minimum points corresponding to each SNR have been used as optimum threshold values in Equation (3.46) and the resulting P_e has been plotted in Fig. 4.12 as P_e vs SNR.

Observe that Equation (3.46) involves the previously encountered parameter m and N , namely the number of correlators used by the receiver. Two different values of each parameter $m = 0, 90$ and $N = 2, 16$ have been used in the computations in order to evaluate their effect on receiver performance. An inspection of Fig. 4.4 ($m = 0, N = 16$) and Fig. 4.6 ($m = 30, N = 16$) reveal that for a given N , m has no significant effect on P_e . On the other hand Fig. 4.4 ($m = 0, N = 16$) and Fig. 4.8 ($m = 0, N = 2$) reveal a small effect of N on P_e for a

given value of m . The actual effect of N on P_e is shown in Fig. 4.12 where P_e has been plotted as a function of SNR for two values of N . Observe that the higher value of N yields better performance. To achieve a P_e of 10^{-4} with $N = 2$, the SNR required is ~ 13.5 dB whereas for the same P_e with $N = 16$ we need an SNR ~ 13.2 dB. This result is once again expected as using few correlators might result in a small output on the correlator branches when $v(t)$ received in $r(t)$ has a delay very much different than the locally generated $v(t)$.

While it is possible to "see" the reason for the independence on m in Equation (3.46), a heuristic explanation of this observed result follows the following argument. The receiver of Fig. 3.1 correlates the incoming signals with local replicas of $v(t)$ delayed by multiples of T/N . Depending on the actual delay in $v(t)$, upon reception of $r(t)$, one of the correlator branches will produce the largest output (or there may be a tie between two branches). The output produced, however, namely which correlator branch is largest, should be independent of the level of uncertainty about λ . Clearly, as m increases, it is easier to predict which correlator branch output will be largest. But this is inconsequential as the receiver is only trying to detect the presence of $v(t)$.

2. Estimator-Correlator Receiver

The second suboptimum receiver analyzed in Chapter III was the Estimator-Correlator of Fig. 3.4. Its performance for $v(t)$ either a periodic sine wave or a square wave was

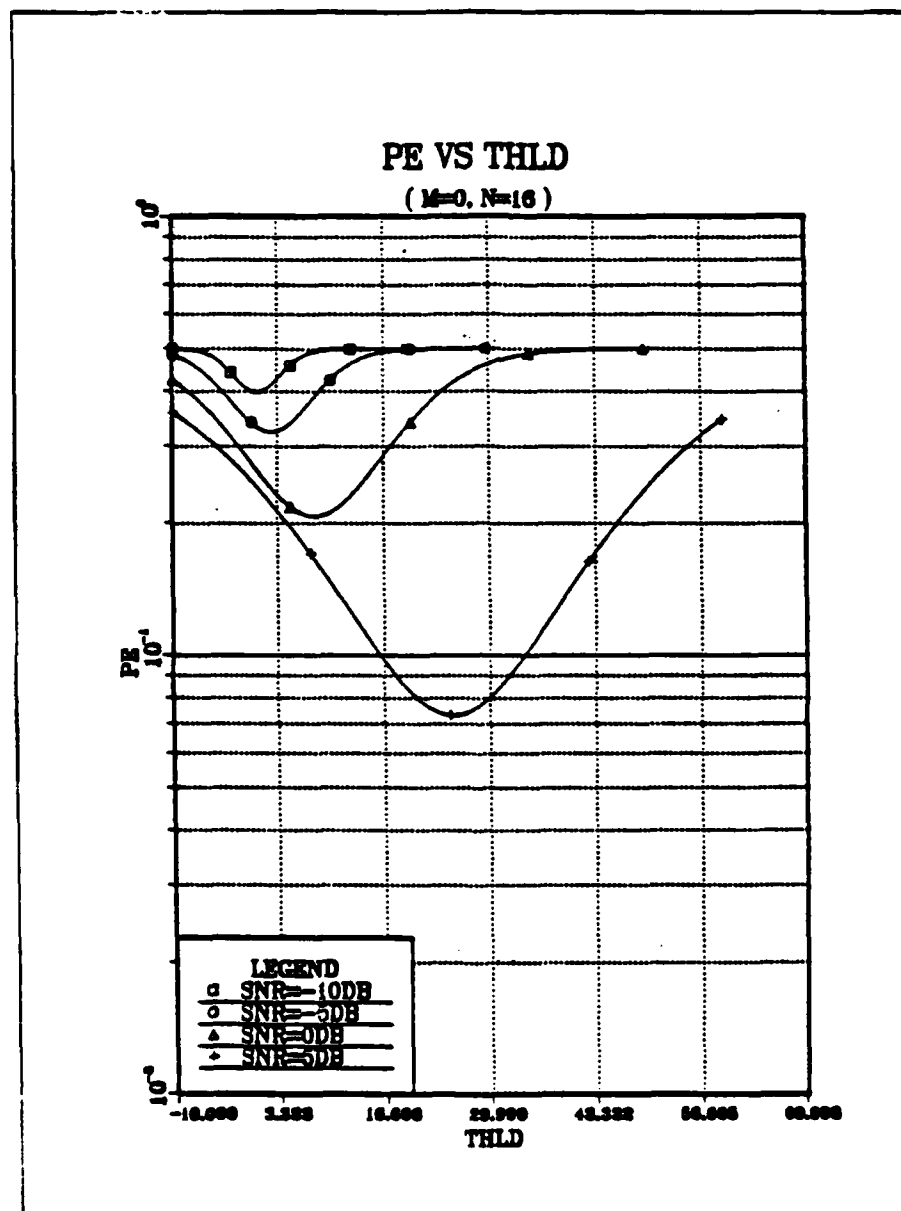


Figure 4.4 P_e vs Thld ($m = 0, N = 16$), (SNR = -10, -5, 0, 5 dB)

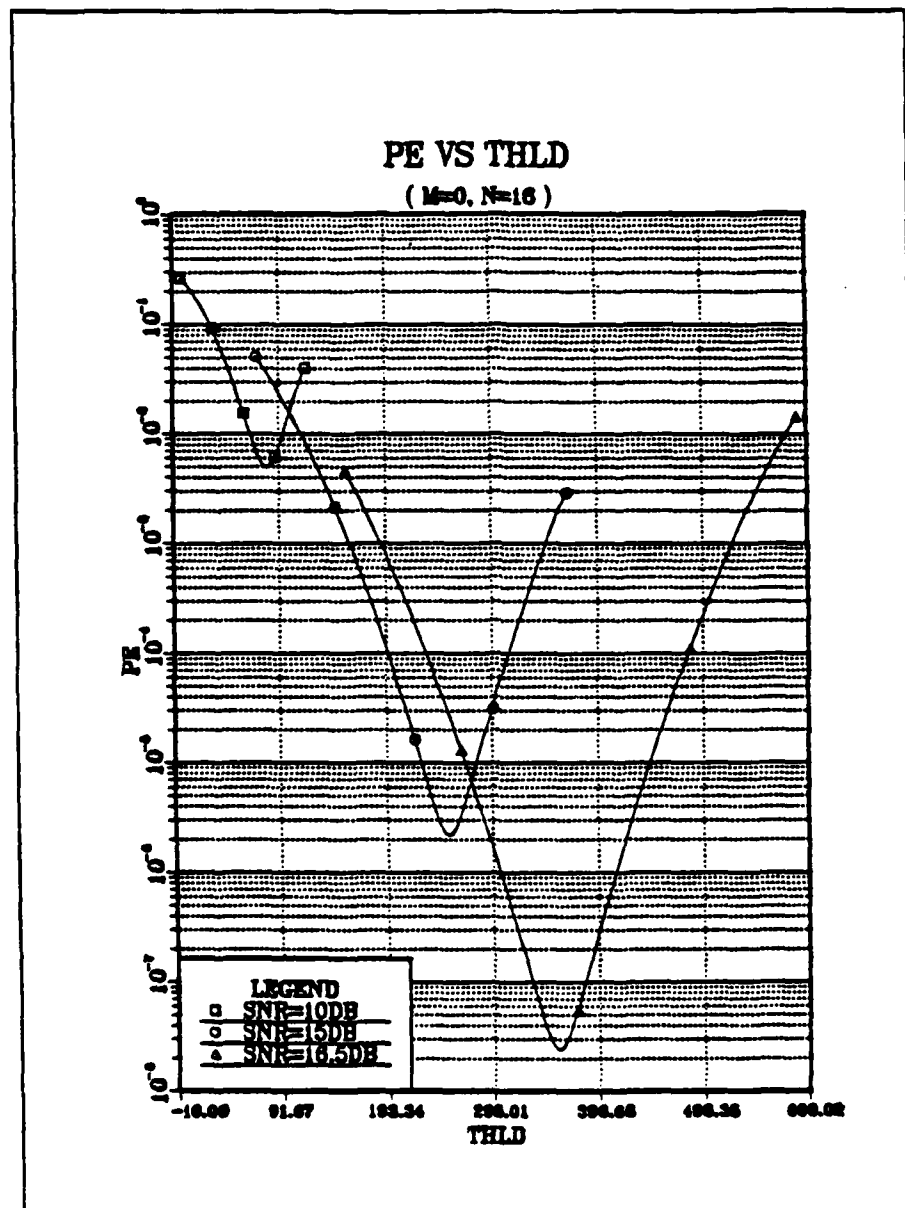


Figure 4.5 P_e vs Thld ($m = 0, N = 16$), (SNR = 10, 15 16.5 dB)

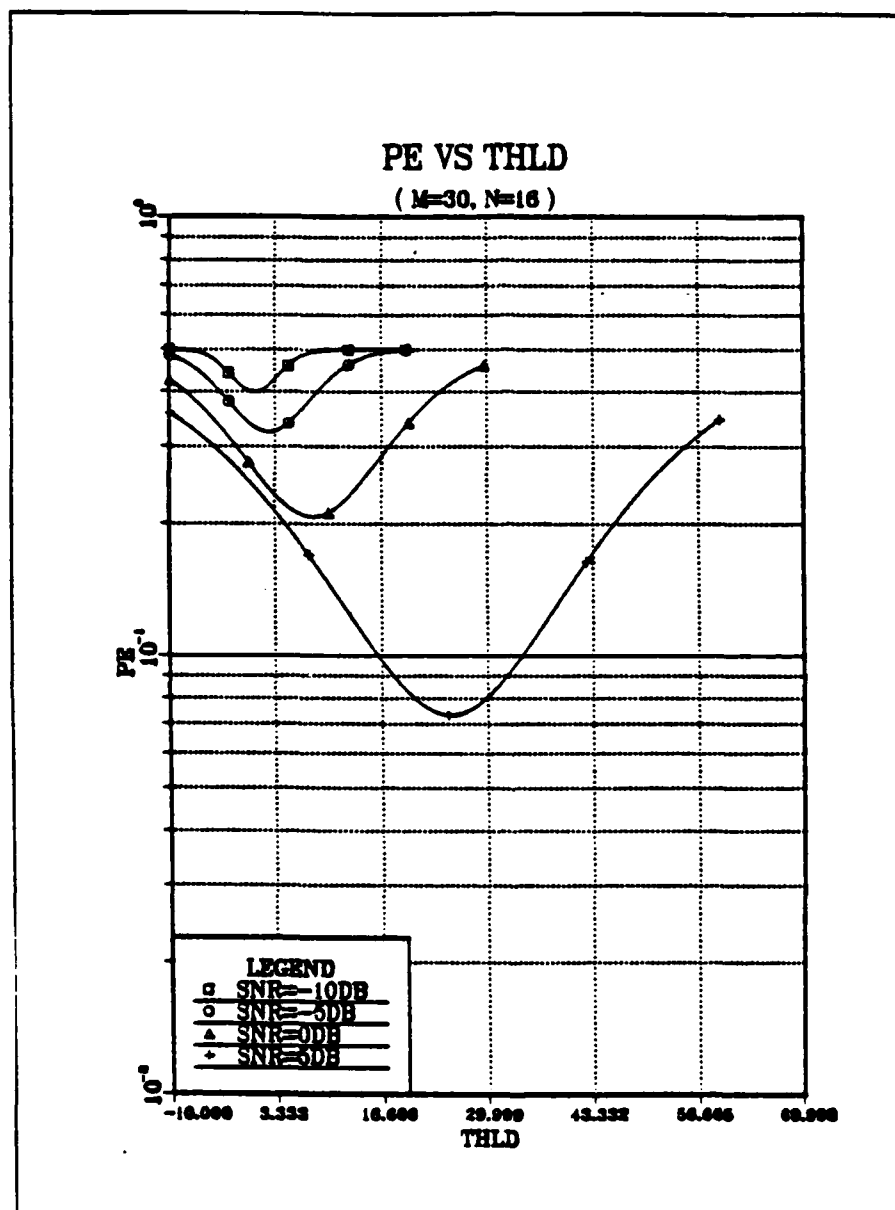


Figure 4.6 P_e vs Thld ($m = 30, N = 16$), (SNR = -10, -5, 0, 5 dB)

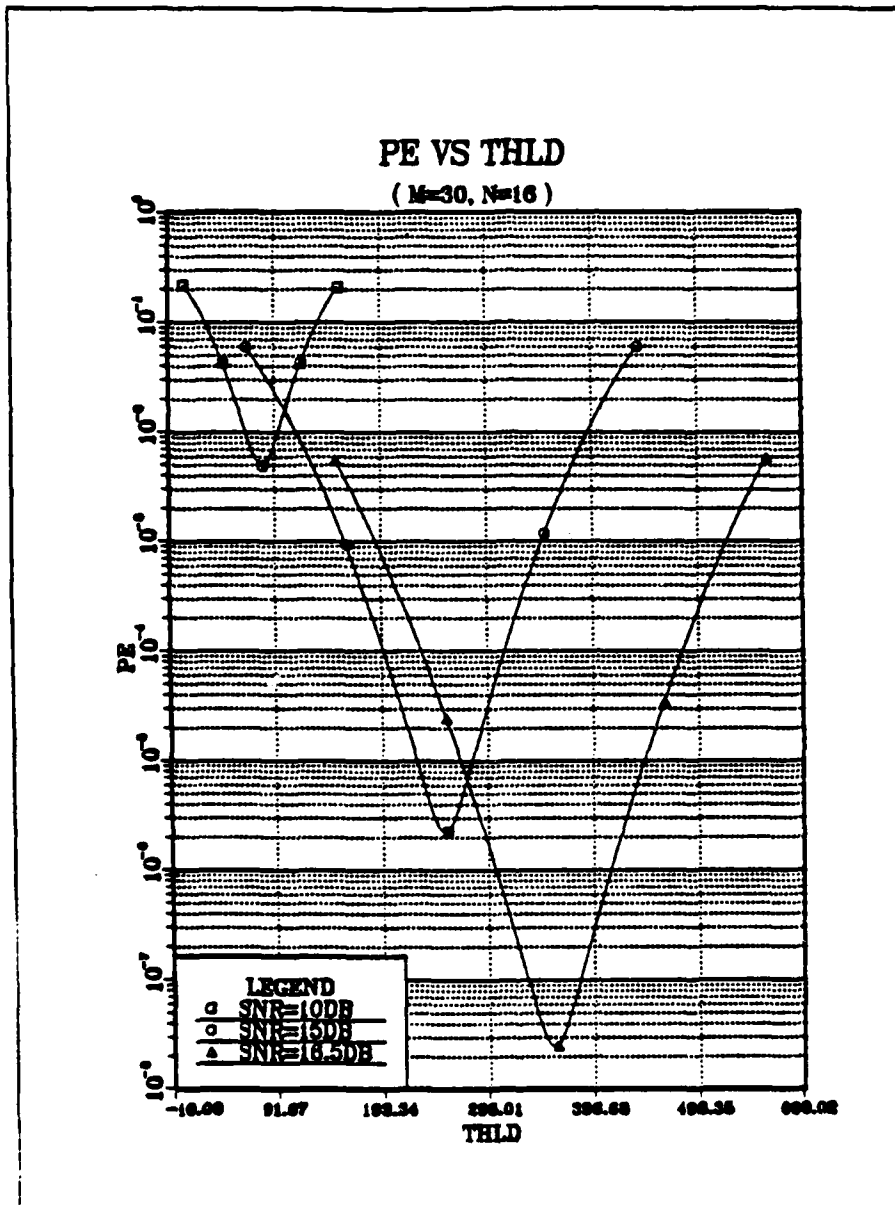


Figure 4.7 P_e vs Thld ($m = 30, N = 16$), (SNR = 10, 15, 16.5 dB)

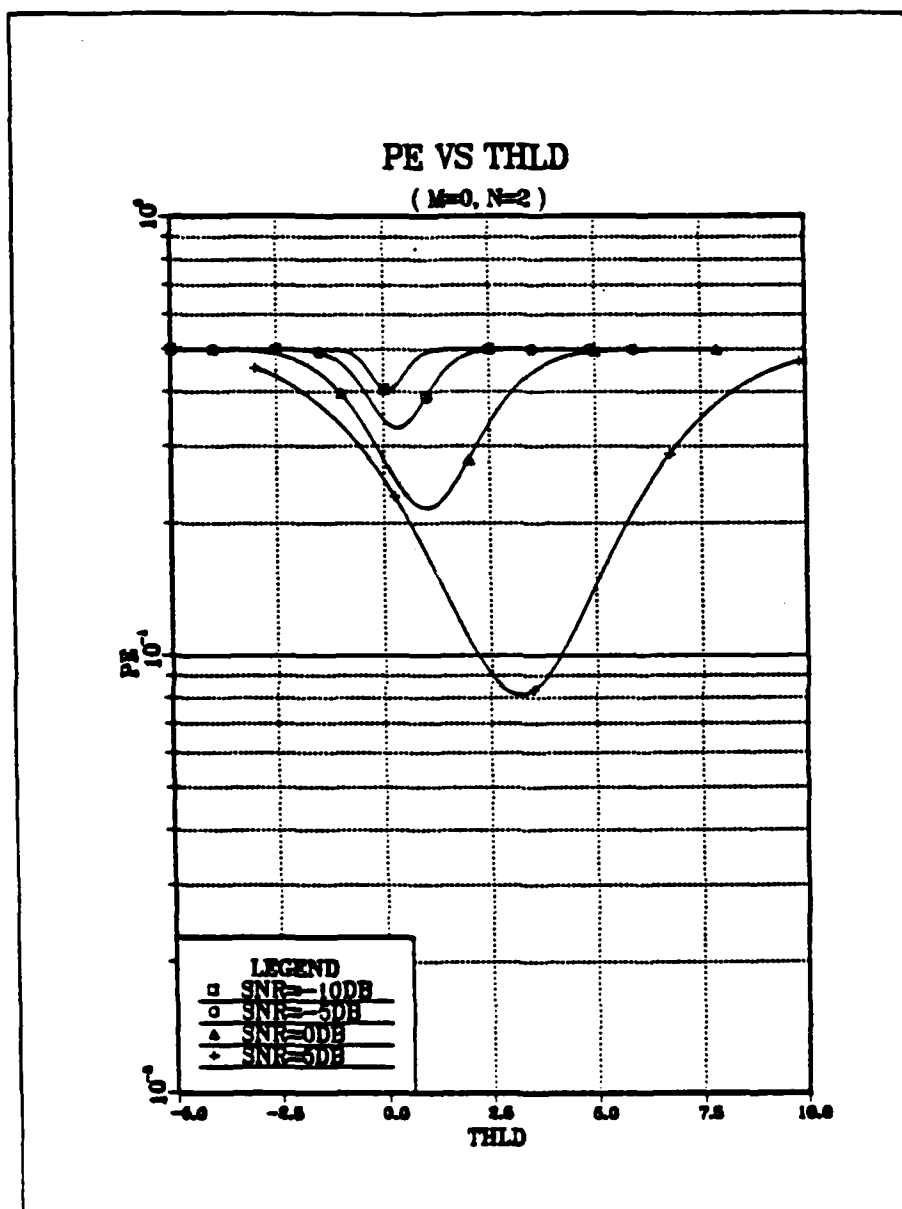


Figure 4.8 P_e vs Thld ($m = 0, N = 2$), (SNR = -10, -5, 0, 5 dB)

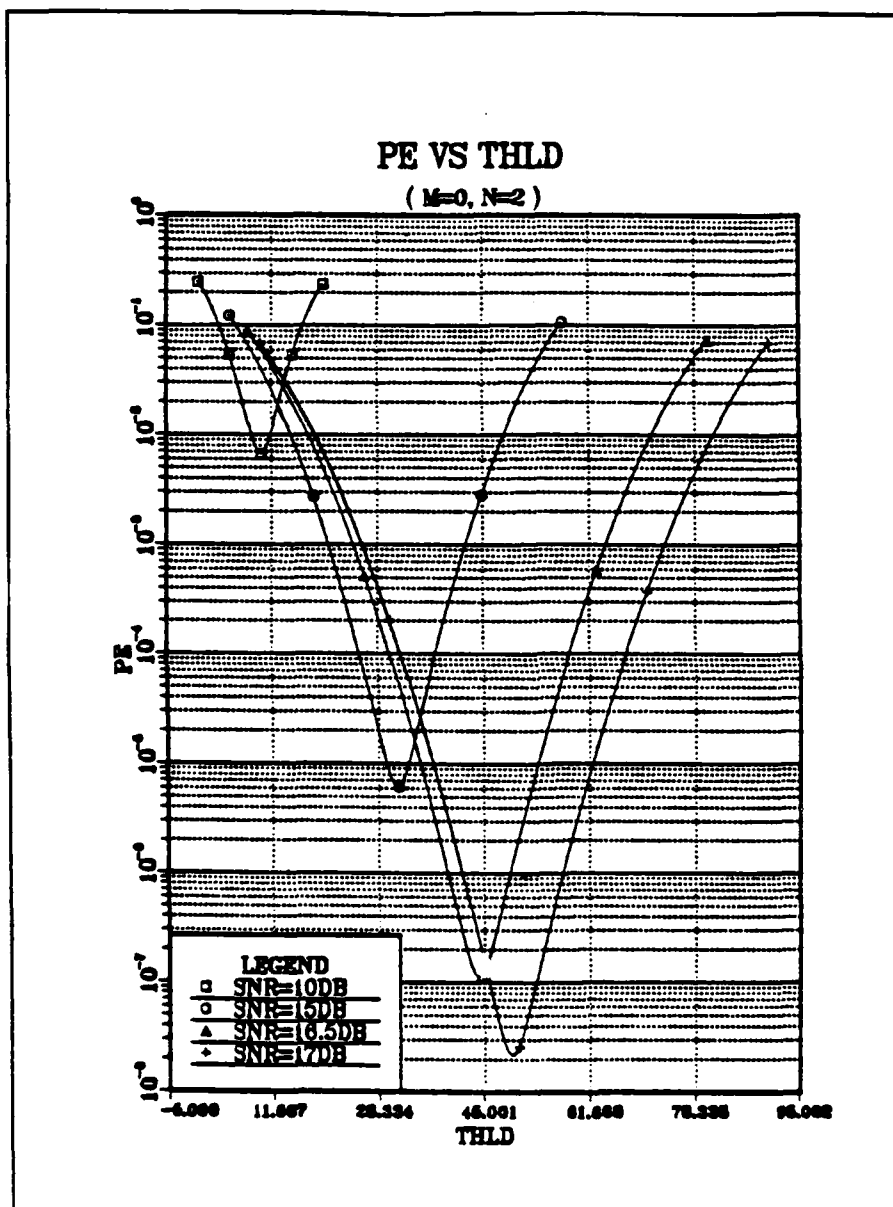


Figure 4.9 P_e vs Thld ($m = 0, N = 2$), (SNR = 10, 15, 16.5, 17 dB)

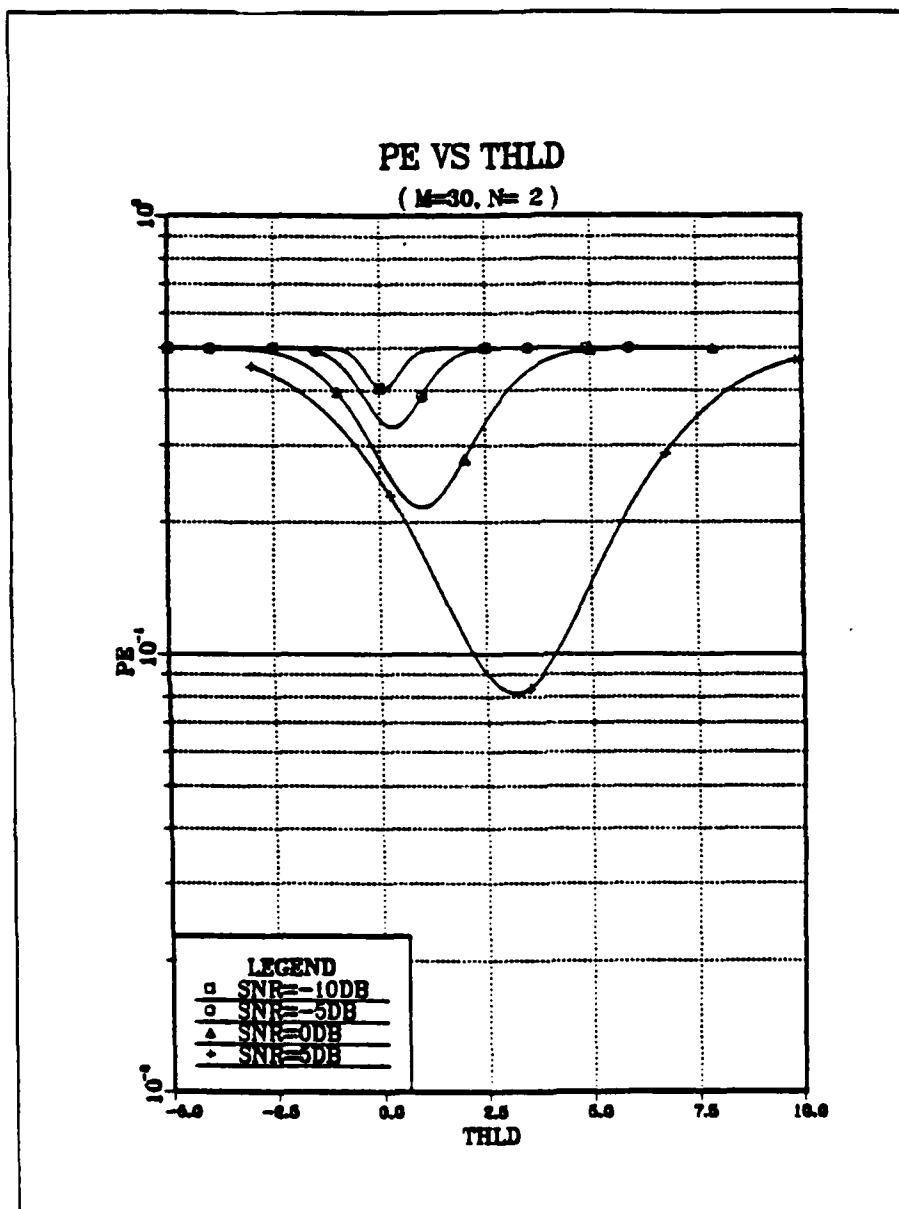


Figure 4.10 P_e vs Thld ($m = 30, N = 2$), (SNR = -10, -5, 0, 5 dB)

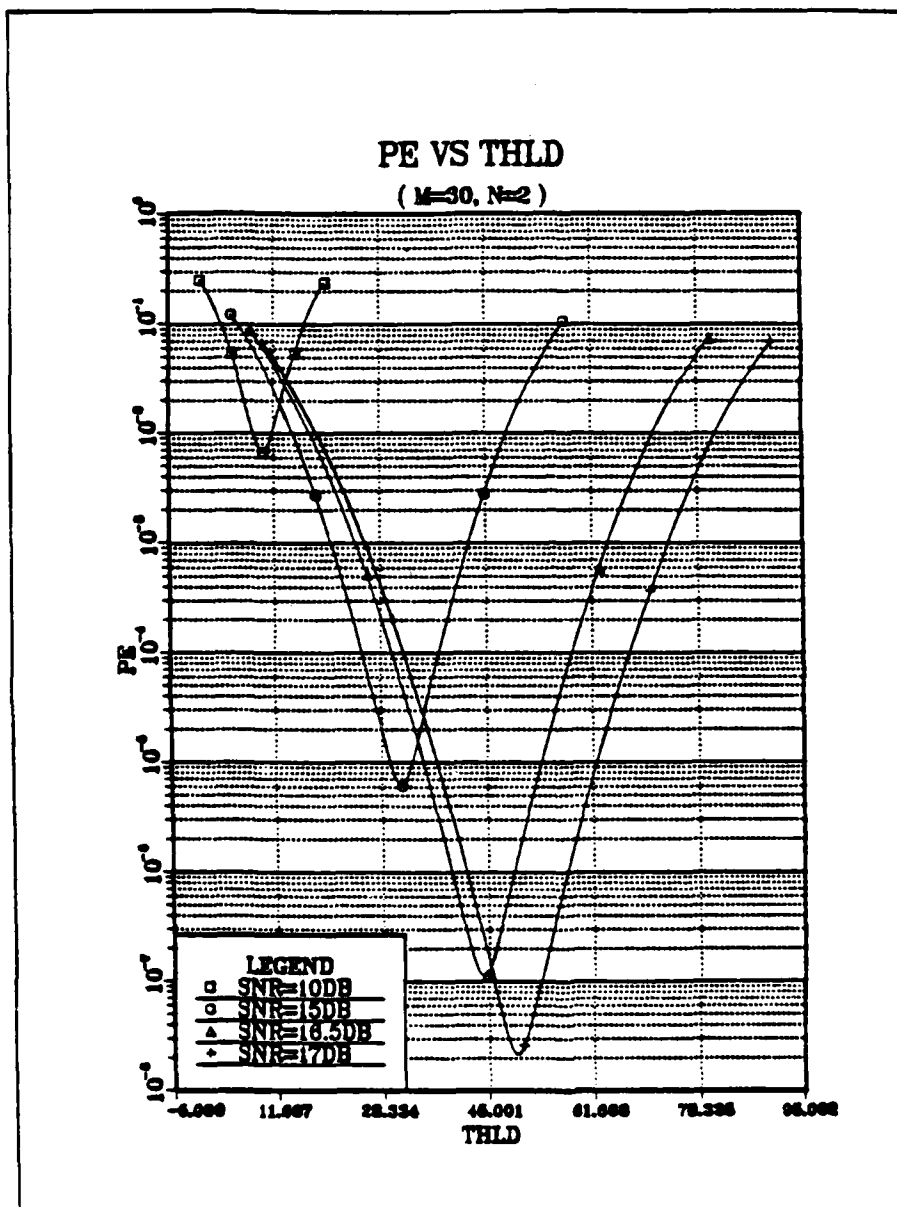


Figure 4.11 P_e vs Thld ($m = 30, N = 2$), (SNR = 10, 15, 16.5, 17 dB)

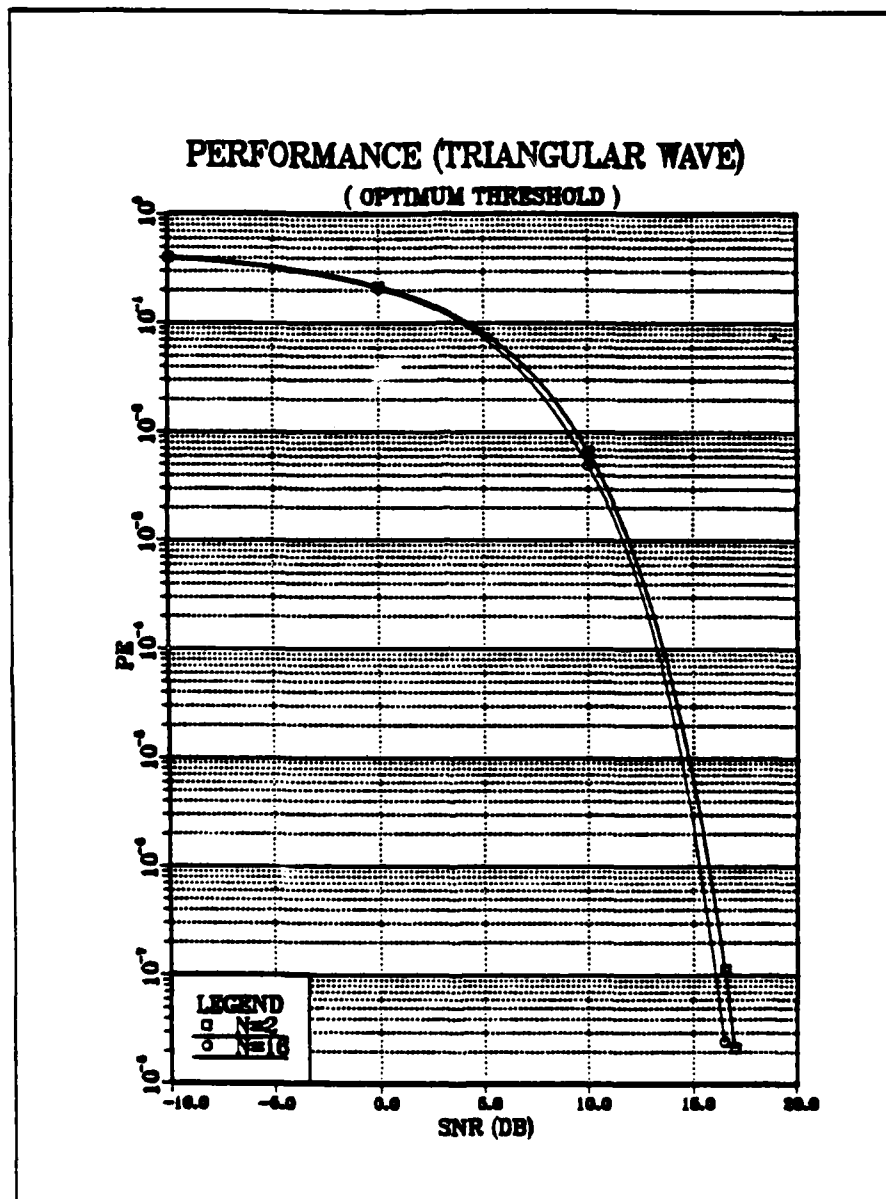


Figure 4.12 Performance (Triangular Pulse).

considered as a function of SNR. As in the case for the N-correlator receiver, this receiver does not have an optimum threshold that is obtained from the theoretical development. However, a procedure similar to that used for the N-correlator receiver has been used to obtain the optimum threshold setting. The P_e has been evaluated as a function of SNR except that here, plots showing P_e as a function of γ have not been included.

Figures 4.13 through 4.16 have been obtained through numerical evaluation of Equations (3.67) and (3.70). Two curves in each figure have been plotted to show the effect of the parameter m on the receiver performance. Observe that Equations (3.67) and (3.69) involve a parameter α which can only take on values iT/N , where $i = 1, 2, \dots, N$. Observe that $i = N$ corresponds to $\alpha = T$ or equivalently $\alpha = 0$ since $v(t)$ is T periodic.

Two values of α have been considered for each of the signals, namely the sine wave and square wave, in order to determine its effect on receiver performance. An inspection of Fig. 4.13 and Fig. 4.14 displaying the performance of the receiver for $v(t)$ a sine wave, or inspection of Fig. 4.15 and Fig. 4.16 displaying the performance of the receiver for $v(t)$ a square wave, it can be observed that α does not have any significant effect on P_e for either case. The logic supporting this observation on receiver performance as a function of α follows from the fact that α is just the estimate of the time delay of the signal, which is obtained by choosing that

correlator branch that produces the largest output. The actual value of α is irrelevant in so far as the performance of the receiver is concerned. The receiver simply uses the estimate of the time delay to produce a decision based on a correlation operation. However, one of the factors that might improve or degrade the error probability is the accuracy of the estimate of the time delay of the signal, which is itself a function of N and SNR.

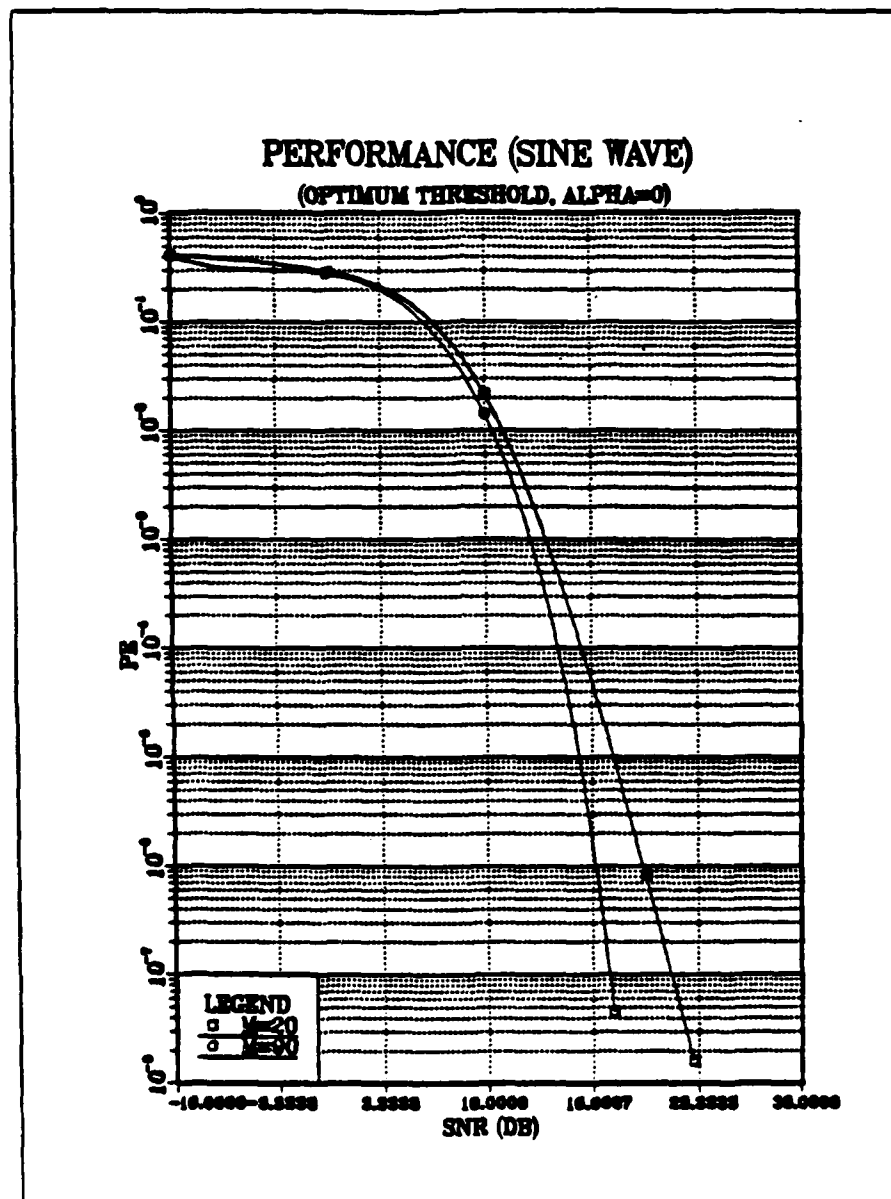


Figure 4.13 Performance (Sine Wave), (Alpha = 0)

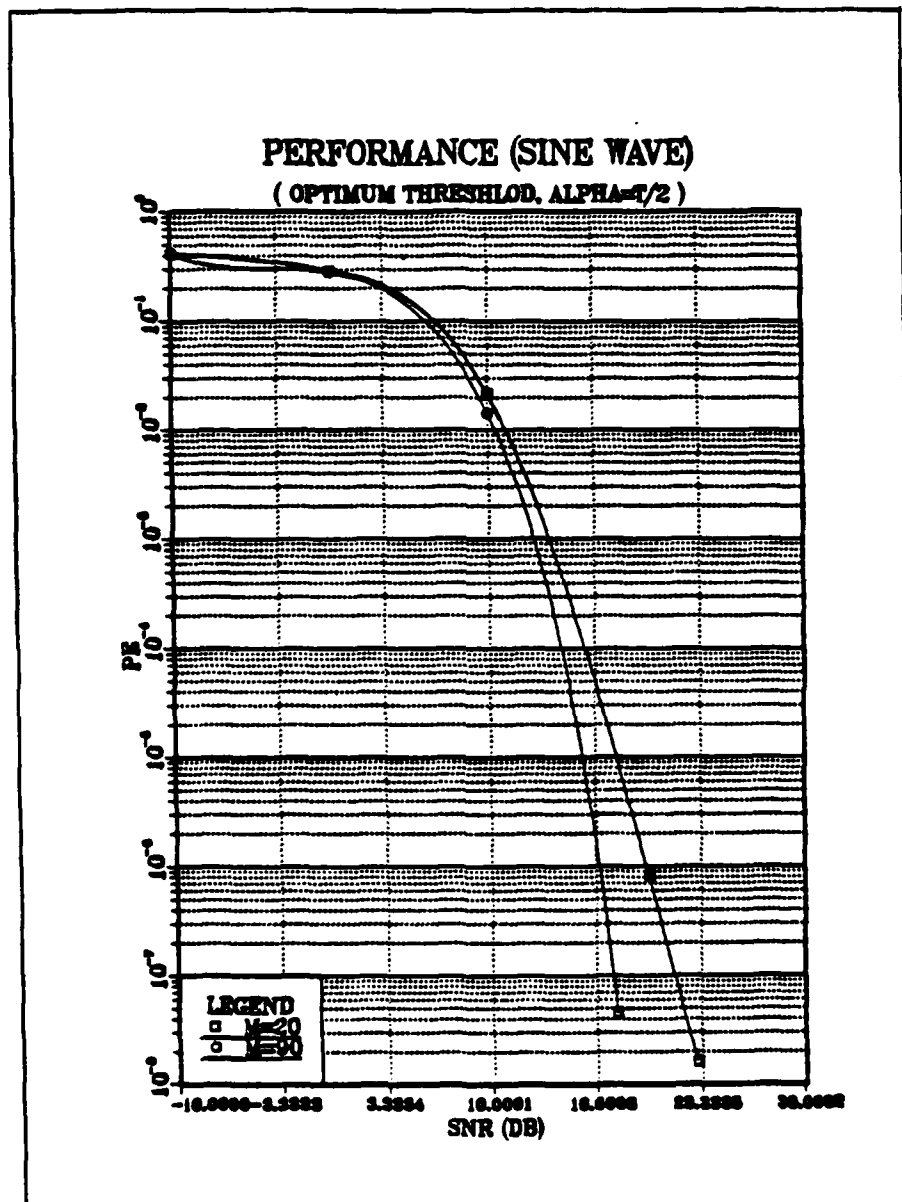


Figure 4.14 Performance (Sine Wave), (Alpha = T/2)

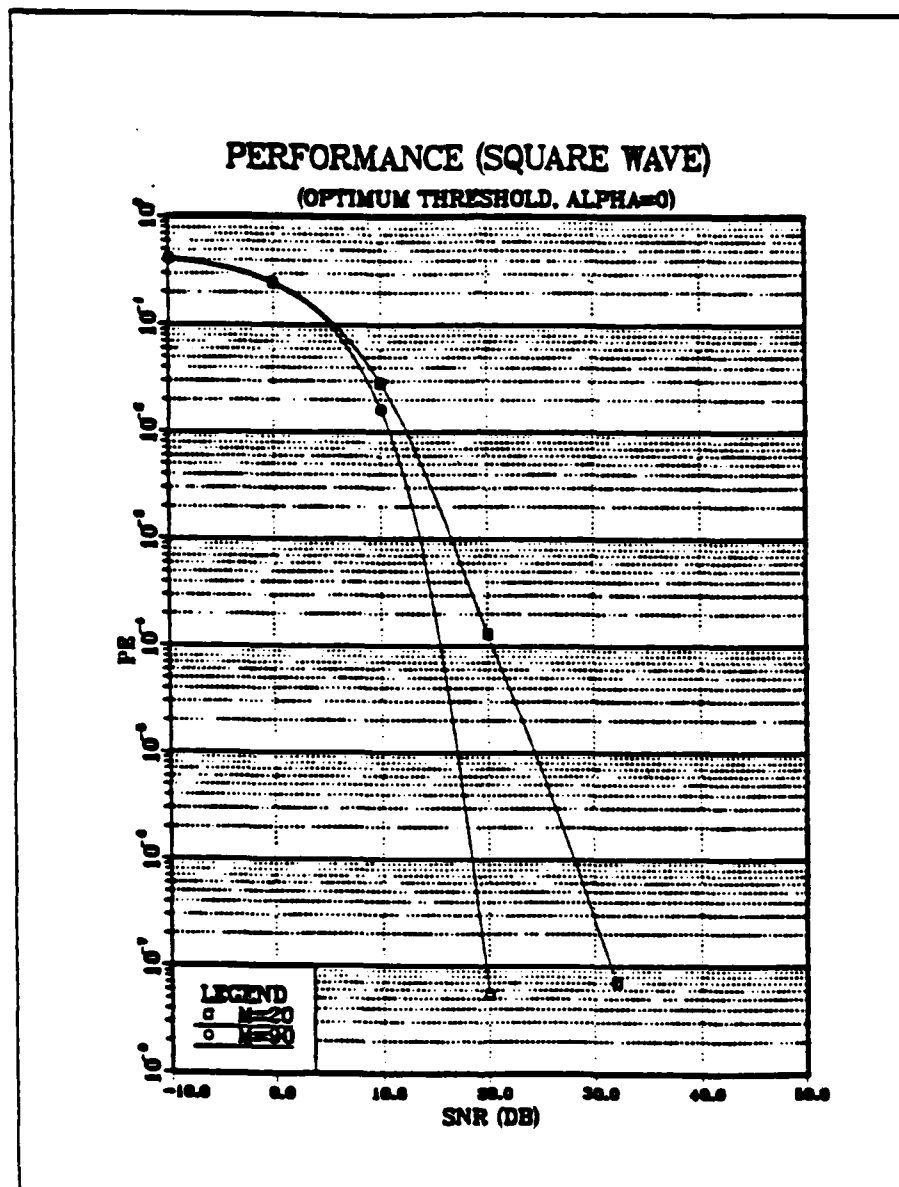


Figure 4.15 Performance (Square Wave), ($\alpha = 0$)

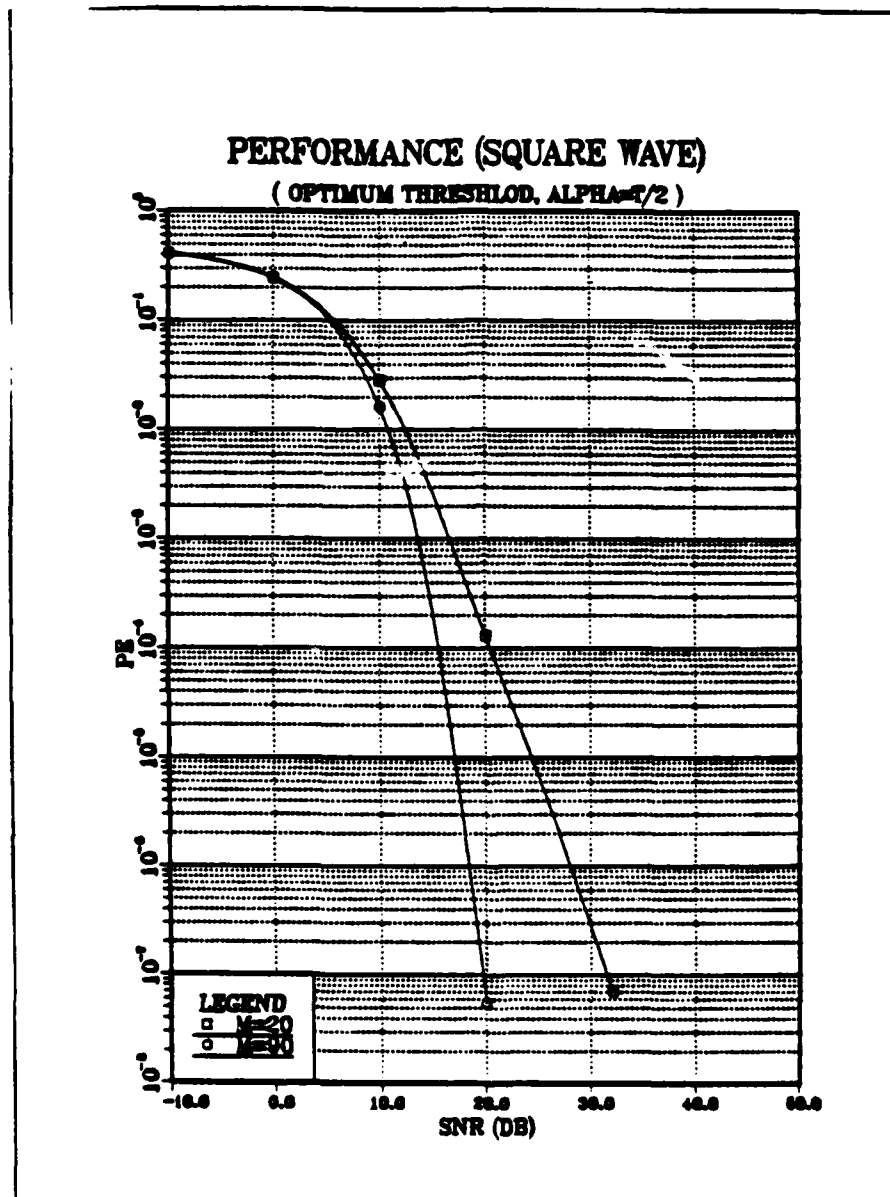


Figure 4.16 Performance (Square Wave), ($\alpha = T/2$)

V. CONCLUSIONS

In this thesis, the analysis and design of noncoherent digital receivers that optimally (and in some cases suboptimally) detect an arbitrarily shaped periodic waveform with random time delay, has been carried out. The probability density function(p.d.f.) of the random time delay λ is assumed to be of some known form. A uniform p.d.f. and a (parameter varying) non-uniform p.d.f. have been considered and their effect on the receiver performance has been studied.

The optimum (in minimum probability of error, P_e , sense) receivers have been designed on the basis of likelihood ratio test under low SNR assumptions. The design of suboptimum receivers is based on heuristic approaches that intuitively yield structures or algorithms that yield good performance.

The analysis carried out in this thesis, allowed for the possibility of unequal prior probabilities of occurrence of the hypotheses, however all examples and computations assumed equal prior probabilities for simplicity.

The low SNR assumption allowed certain mathematical complexities to be overcome. Therefore graphical results involving the performance (P_e) of optimum receivers are valid and therefore presented only for SNR values less than or equal to -4 dB. Operating at SNR values less than or equal to 0 dB is the basic requirement of covert communication and may also be necessary in certain radar applications.

The optimum receiver operating on the signals that have non-zero DC component, detects the signal with higher level of error probability and it decreases with the increase of SNR as expected. While it is clear that no receiver could operate with such an undesirable level of error probability, the graph displaying the performance (P_e) does give an indication of the performance level that can be expected at low SNR's. In the region of high SNR, it is expected that error probability will continue to decrease to reasonable levels. However, for high SNR's this receiver is no longer optimum.

The second optimum receiver operating on arbitrary signals does also yield poor performance. But here again we must not forget that the receiver is operating in the low SNR region. The graphs displaying the performance of this receiver for the sine wave and square wave give an indication of the performance that can be expected at low SNR's. Also, they reveal an improvement in the performance with an increase in the parameter m . It is concluded that for high SNR's, this receiver is also no longer optimum.

One of the receivers designed via heuristic means was a (suboptimum) N-correlator receiver. Its performance was derived and tested for the case in which $v(t)$ was a periodic triangular waveform. While this receiver is unable to detect a sine wave, it is capable of detecting a square wave or some other periodic waveform. The other receiver designed via heuristic means, namely the Estimator-Correlator receiver, was analyzed in terms of its P_e as a function of SNR.

From the graphical results of the performance of the N-correlator receiver, it is concluded that receiver performance gets better as N, the number of correlators, gets bigger. It is further concluded that m, the parameter that determines the uncertainty about the time delay λ , does not have any effect on the receiver performance. In general, it was observed that except for the case of the N-correlator receiver, the parameter m had a significant effect on the performance of the receivers.

While a number of practical problems have been addressed in this thesis, related problems and potential studies abound. For example, the receiver obtained using a three-term approximation in the exponential of Equation (2.19) needs to be analyzed further in terms of performance for both uniform and non-uniform p.d.f. on λ . Furthermore, other (suboptimum) receivers need to be proposed and analyzed, such as simple energy detection receivers.

APPENDIX A

DERIVATION OF MEAN AND VARIANCE OF R.V. λ

The p.d.f. of r.v. λ (time delay) given by Equation (2.1) is

$$f_{\Lambda}(\lambda; m) = \frac{e^{m \cos \frac{2\pi}{T}\lambda}}{T I_0(m)} \quad \lambda \leq |T/2|, \quad 0 \leq m \leq \infty \quad (\text{A.1})$$

Substitution of Equation (2.41) into Equation (A.1) yields

$$f_{\Lambda}(\lambda; m) = \frac{\sum_{p=-\infty}^{\infty} I_p(m) \cos p \frac{2\pi}{T}\lambda}{T I_0(m)} \quad \lambda \leq |T/2|; \quad 0 \leq m \leq \infty \quad (\text{A.2})$$

so that the expected value or mean of r.v. λ can be expressed as

$$\begin{aligned} E\{\lambda\} &= \int_{-T/2}^{T/2} \lambda f_{\Lambda}(\lambda; m) d\lambda \\ &= \frac{1}{T I_0(m)} \sum_{p=-\infty}^{\infty} I_p(m) \int_{-T/2}^{T/2} \cos(p 2\pi \lambda / T) d\lambda \\ &= 0 \end{aligned} \quad (\text{A.3})$$

since the product of λ (odd function) and $\cos(p2\pi\lambda/T)$ (even function) is an odd function and integral of an odd function produces zero.

The variance of λ is given by

$$\begin{aligned} E\{\lambda\}^2 &= \int_{-T/2}^{T/2} \lambda^2 f_{\Lambda}(\lambda; m) d\lambda \\ &= \frac{1}{T I_0(m)} \int_{-T/2}^{T/2} \lambda^2 e^{m \cos 2\pi\lambda/T} d\lambda \end{aligned} \quad (A.3)$$

since we have a zero mean random variable.

The variance is clearly a function of m . However, the integral of Equation (A.3) is not readily evaluated in closed form. The computer has been used to evaluate

$$\frac{\text{Var}\{\lambda\}}{T^2} = \frac{1}{4 I_0(m)} \int_0^1 x^2 e^{m \cos \pi x} dx \quad (A.4)$$

and it has been clearly demonstrated that $\text{Var}\{\lambda\}/T^2$ becomes smaller as m grows.

APPENDIX B

INTERPRETATION OF A SMALL EXPONENTIAL IN EQUATION (2.22) AND EQUATION (2.60)

In Equation (2.22) and Equation (2.60) it has been assumed that

$$\frac{2}{N_0} \int_0^{T_0} r(t)v(t-\lambda)dt \triangleq \varepsilon \ll 1 \quad (B.1)$$

This appendix is devoted to analyzing under what conditions is this assumption valid. Observe that ε is a r.v. so that Equation (B.1) must be analyzed in a statistical sense. Recall that

$$E\{\varepsilon|H_0\} = 0 \quad (B.2)$$

since the noise has been assumed to be zero mean and

$$E\{\varepsilon|H_1\} = \frac{2}{N_0} \int_0^T v^2(t-\lambda) = \frac{2}{N_0} E \quad (B.3)$$

where E is the signal energy for $0 \leq t \leq T_0$.

Thus, provided $E/N_0 \ll 1$, ε under either hypothesis on the average takes the value zero or a value close to it. The excursions of ε away from the mean can be obtained by evaluating the conditional variances. Since

$$\begin{aligned}
E\{\epsilon^2 | H_0\} &= E\left\{\left[\frac{2}{N_0} \int_0^{T_0} n(t) v(t-\lambda) dt\right]^2\right\} \\
&= \frac{4}{N_0^2} \int_0^{T_0} \int_0^{T_0} E\{n(t)n(\tau)\} v(t-\lambda)v(\tau-\lambda) dt d\tau \\
&= \frac{2}{N_0} \int_0^{T_0} v^2(t-\lambda) dt = \frac{2}{N_0} E
\end{aligned} \tag{B.4}$$

and

$$\begin{aligned}
E\{\epsilon^2 | H_1\} &= E\left\{\left[\frac{2}{N_0} \int_0^{T_0} v^2(t-\lambda) dt + \frac{2}{N_0} \int_0^{T_0} n(t)v(t-\lambda) dt\right]^2\right\} \\
&= E\left\{\left(\frac{2E}{N_0}\right)^2 + 2\left(\frac{4}{N_0^2} \int_0^{T_0} n(t)v(t-\lambda) dt\right) \right. \\
&\quad \left. + \left(\frac{2}{N_0} \int_0^{T_0} n(t)v(t-\lambda) dt\right)^2\right\} \\
&= \left(\frac{2E}{N_0}\right)^2 + \frac{2E}{N_0}
\end{aligned} \tag{B.5}$$

Thus

$$\text{Var}\{\epsilon | H_0\} = \frac{2E}{N_0} = \text{Var}\{\epsilon | H_1\} \tag{B.6}$$

Therefore, provided that $E/N_0 \ll 1$, ϵ remains very close to its average value which is either zero or very close to zero. Note also that in a more rigorous sense, we can bound

$$P\{\epsilon^2 \geq \delta | H_1\} \leq \frac{E\{\epsilon^2 | H_1\}}{\delta} \quad (B.7)$$

If we set $\delta = 1$, then

$$P\{\epsilon^2 \geq 1 | H_0\} \leq \frac{2E}{N_0} \quad (B.8)$$

and

$$P\{\epsilon^2 \geq 1 | H_1\} \leq \left(\frac{2E}{N_0}\right)^2 + \frac{2E}{N_0} \quad (B.9)$$

In both cases if $2E/N_0 \ll 1$, then $P\{\epsilon \geq 1 \text{ or } \epsilon \leq -1\}$ is also small. Therefore, a small E/N_0 guarantees that the assumption of a small exponential in Equations (2.22) and (2.60) is valid with a high degree of probability.

LIST OF REFERENCES

1. Wainstein, L. and Zubakov, V., Extraction of Signals from Noise, Englewood Cliffs, N.J., Prentice-Hall, 1962.
2. Gagliardi, R.M., "Noncoherent Detection of Periodic Signals," IEEE Trans. Information Theory, Vol. IT-21, pp. 282-285, May 1975.
3. Srinath, M.D. and Rajasekaran, P.K., An Introduction to Statistical Signal Processing with Applications, John Wiley, 1979.
4. Whalen, A.D., Detection of Signals in Noise, Academic Press, 1971.
5. Abramowitz, M. and Stegun, I.E., Handbook of Mathematical Functions With Formulas, Graphs, and Mathematical Tables, U.S. Department of Commerce, National Bureau of Standards, 1972.

INITIAL DISTRIBUTION LIST

	No. Copies
1. Defense Technical Information Center Cameron Station Alexandria, Virginia 22304-6145	2
2. Library, Code 0142 Naval Postgraduate School Monterey, California 93943-5100	2
3. Prof. D. Bukofzer, Code 62Bh Naval Postgraduate School Monterey, California 93943-5100	5
4. Prof. J.F. Chang, Code 62Cn Naval Postgraduate School Monterey, California 93943-5100	1
5. Prof. Harriet B. Rigas, Code 62 Naval Postgraduate School Monterey, California 93943-5100	1
6. LT Khalil A. Ansari Ansari Mohalla, Hala (New) Sind Pakistan	2
7. Lt Sarfraz Hussain SMC #1206 Naval Postgraduate School Monterey, California 93943-5100	1